論文 / 著書情報
Article / Book Information

題目(和文)	V-Fe-O系の相平衡および関連物質の熱力学的および磁気的性質
Title(English)	Phase Equilibria of the V-Fe-O System and Thermodynamic and Magnetic Properties of the Related Compounds
著者(和文)	脇原將孝
Author(English)	Masataka Wakihara
出典(和文)	学位:理学博士, 学位授与機関:東京工業大学, 報告番号:甲第417号, 授与年月日:1971年3月26日, 学位の種別:課程博士, 審査員:桂敬
Citation(English)	Degree:Doctor of Science, Conferring organization: Tokyo Institute of Technology, Report number:甲第417号, Conferred date:1971/3/26, Degree Type:Course doctor, Examiner:
学位種別(和文)	博士論文
Type(English)	Doctoral Thesis

大学院博士論文

V-Fe-O系の相平衡と関連物質の熱力学的および磁気的性質

化学専攻

脇原将孝

8036

（指導教官　柱　敬　教授）

Phase Equilibria of the V-Fe-O System and Thermodynamic and Magnetic Properties of the Related Compounds

1971

MASATAKA WAKIHARA

Department of Chemistry, Tokyo Institute of Technology

CONTENTS

GENERAL INTRODUCTION

Vanadium is a minor element in the earth's crust, and the essentials of the geochemistry of vanadium in lithosphere are fairly well known, that is to say, geochemists believe that the distribution of trivalent vanadium in the magmatic rocks including basalt to rhyolite is in oxygen compounds, and here vanadium is associated with trivalent iron especially in magmatic magnetite, Fe_3O_4. Indeed, vanadium is usually concentrated in titanomagnetite crystallized from magmatic state, and it seems to be reasonable that vanadium in magmatic state is in trivalent state on the basis of the ionic radii because the ionic size of trivalent vanadium follows closely ferric iron, and the radius of trivalent vanadium, 0.65 Å, being only slightly less than that of ferric iron, 0.67 Å. Turning to the ionic picture, vanadium appears with various charges changing from +2 to +5. In fact, there are many compounds in the V-O system and the stabilities of these vanadium oxides at a certain temperature depend on the oxygen fugacity. Particularly, many compounds which may be described by the general formula V_nO_{2n-1} ($n \geqq 2$) have been reported in the V_2O_3-VO_2 system. Nevertheless, the phase relations found in the V_nO_{2n-1} series and their thermodynamic data have not yet been completely established especially at high temperature because of the difficulty to determine the stability ranges of oxygen partial pressure at each phase. Under these con-

siderations, it is, therefore, quite desirable to obtain accurate phase equilibria in the V-O system, which, of course, are in chemical equilibrium in order to focus the light from the stand point of oxygen partial pressure on the geochemical behaviour of vanadium in magmatic state.

The phase equilibria and thermodynamic data on the Fe-O system have been precisely determined by many investigators and applying these results, the Fe-Cr-O and the Fe-Ti-O systems have been studied. However, a few studies of the phase equilibria on the Fe-V-O system have been reported only at pretty lower temperatures compared with magmatic ones, and almost all of these studies were based on non-criteria about equilibrium state. Some investigators pointed out the existence of many homogeneous solid solution series and compounds in this system at high temperatures. It seems to be important in order to clarify the descriptive conclusion found in magmatic magnetite to establish the phase equilibria in the Fe-V-O system at high temperatures. The results studied on this line may contribute not only on geochemistry but also on many fields including thermochemistry.

CHAPTER 1

Phase Equilibria and Thermodynamic Properties of the V_2O_3-V_4O_7 System at Temperatures from 1400° to 1700°K

1-1 INTRODUCTION

A large number of intermediate oxide phases have been reported in the V-O system. Klemm and Grimm[1] studied the phase relations in the V-V_2O_3 system. They found that the VO phase with compositions ranging from $VO_{0.9}$ to $VO_{1.3}$ was stable at high temperature side, while it decomposes to metallic vanadium and a higher oxide (not V_2O_3) at low temperature. Seybolt and Sumsion[2] reported the existence of a metallic oxide with the approximate limits of homogeneity $VO_{0.15}$-$VO_{0.25}$. Hoschek and Klemm[3] who first studied V_2O_3-V_2O_5 system, suggested the presence of the five phases of V_2O_3, β-phase ($VO_{1.65}$-$VO_{1.80}$), α-phase ($VO_{1.80}$-$VO_{2.00}$), α'-phase ($VO_{2.05}$-$VO_{2.33}$) and V_2O_5, respectively. They also stated that α-phase has a structure of rutile type and is homogeneous between $VO_{1.8}$ and $VO_{2.0}$. Aebi[4] found a new phase with the composition of $VO_{2.17}$ at 600°C. Lately, Andersson[5] studied in detail the V_2O_3-VO_2 system at temperatures from 800° to 900°C and identified eight intermidiate phases represented by the general chemical formula V_nO_{2n-1}, changing n's number from 2 to 8. The homogeneous V_nO_{2n-1} ($n \geq 2$) series are sometimes

called Magnéli phases after the main investigator. Their structures were investigated by G. Andersson[6] and S. Andersson et al[7]. Kosuge et al.[8] recognized V_2O_3, V_3O_5, V_4O_7, V_5O_9, V_6O_{11} and V_7O_{13} phases at 800°C and measured the magnetic properties of their compounds. Kosuge[9] recently recognized their phases by measuring the magnetic susceptibility and Mössbauer effect and presented a general phase diagram of V_2O_3-V_2O_5 system up to 1200°C together with the data of Kachi and Roy[10]. As described above, there are rather numbers of studies on the V_2O_3-VO_2 system at low temperature side. On the other hand, only a few papers are known about the phase equilibria and thermochemical properties on the V_2O_3-VO_2 system at high temperature side except for V_2O_3 and VO_2[11]. Katsura and Hasegawa[12] reconfirmed the phase equilibria studied by Andersson[5] and Burdese[13] and Grossmann et al[14]. and presented the standard free energies of compounds which exist in the V_2O_3-VO_2 system at 1600°K. Recently, Anderson and Khan[15] studied the V_2O_3-VO_2 system up to 1423°K and reported some thermodynamic data of the system.

The object of the present study is to investigate the phase equilibria in the V_2O_3-V_4O_7 system in detail by varying temperatures from 1400° to 1700°K, and also to present some thermodynamic considerations, particularly the standard free energies of oxidation of vanadium oxides, V_2O_3 and V_3O_5.

1-2 EXPERIMENTAL

1-a) General Procedure ——— Different experimental methods were used in the present study- quenching and thermogravimetric methods previously described by Katsura and Muan[16] and by Katsura and Kimura[17].

In the thermogravimetric method, the guaranteed reagent of ammonium meta vanadate was gently heated at 450°C in globar to obtain V_2O_5; then V_2O_5 was loosely pressed into a small size crucible and heated at 650°C to make a suitable pellet of oxide in an electric furnace while passing a mixed gas of CO_2/H_2 = 1 through the heating tube for one hour. About 2 grams of pellet thus obtained had a chemical formula of approximate V_2O_3 phase. The pellet was made several holes by a needle to make the sample easily attaining the equilibrium. The sample was suspended in a vertical tube by a thin platinum-40% rhodium wire from the lower part of quick weighing balance. The weight changes were recorded as a function of the oxygen partial pressure at any constant temperature. The data thus obtained were used to locate the oxygen isobars.

In the quenching method, a pellet of oxide sample which was held by a thin platinum wire was heated at any constant temperature and at a chosen oxygen partial pressure until equilibrium was attained between the gas and the solid phases. The sample was then quenched rapidly to the temperature of cold water by burning away the thin platinum wire with an

electric current. The sample thus obtained were used for determining the phases present by X-ray and for the determination of the composition by chemical analysis.

1-b) Choice of the Reference State for the Chemical Composition ——— During the preliminary studies, it was recognized that the composition of the V_2O_3 phase remained accurately stoichiometric over a wide range of the oxygen partial pressure at temperatures from 1400° to 1700°K. In addition, the chemical analysis of the quenched samples obtained from the range of oxygen partial pressure 10^{-11} to 10^{-14} atm. had the stoichiometric composition of $VO_{1.500}$ within the experimental error. Therefore, the composition $VO_{1.500}$ was chosen as the reference weight standard in the thermogravimetric method.

1-c) Determination of the composition by the thermogravimetric method ——— A composition at any oxygen partial pressure was determined by measuring weight changes between the stoichiometric V_2O_3 (reference state) and a certain more oxidized composition according to the following equations;

$$VO_{1.500} + x/2\ O_2 = VO_{1.500} + x \qquad (1)$$

$$x = \frac{M_{VO_{1.5}}}{M_o} \cdot \frac{(b-a)}{a} = 4.684 \cdot \frac{(b-a)}{a} \qquad (2)$$

where a is the weight of stoichiometric V_2O_3 phase (reference

state) and B indicates the weight at any equilibrated oxygen pressure. $M_{VO_{1.5}}$ and M_o are formula weight of V_2O_3 and O_2, respectively.

1-d) Control of the Atmosphere ——— A desired partial pressure of oxygen was obtained by using a gas mixture of CO_2 and H_2. The CO_2-H_2 mixtures were prepared by proportioning the two gas components in desired ratios in a gas mixer which is similar in principle to that used by Darken and Gurry[18]. The fluctuation of the CO_2/H_2 ratio was estimated to be within ± 1 per cent throughout the present study. The purity of the carbon dioxide and hydrogen used in the present study was sufficient for the present purposes.

1-e) Calculation of the Oxygen Partial Pressure ——— An oxygen partial pressure, which was obtained by mixing CO_2 and H_2 gases, was calculated by the free energy data of Elliott and Gleiser[19] as follows;

$$CO_2 + H_2 \overset{K_1}{=} CO + H_2O \qquad (3)$$

$$CO_2 \overset{K_2}{=} CO + 1/2\ O_2 \qquad (4)$$

where K_1 and K_2 are equilibrium constants of Eq.(3) and Eq. (4), respectively.

An oxygen partial pressure (Po_2) was calculated by using

following equation based on values of K_1 and K_2;

$$Po_2^{1/2} = K_2/2 \left[\sqrt{(a-1)^2 + 4a/K_1} + (a-1) \right] \qquad (5)$$

where a is the initial ratio of CO_2 to H_2 at room temperature.

1-f) Correction of Oxygen Partial Pressure ——— The calculated partial pressure of oxygen is necessary to correct because of the difference of diffusion between CO_2 and H_2 in a furnace tube, and unaccuracy of CO_2/H_2 ratio more than CO_2/H_2 = 200. Therefore, a solid electrolyte cell tube composed of stabilized zirconia $(ZrO_2)_{0.85}(CaO)_{0.15}$ was used to correct the calculated oxygen partial pressure.

The principles of this electrolyte for the determination of the oxygen partial pressure and the design for the general utility have been published[20-24] and some precise results have been reported[12)25-28]. The $(ZrO_2)_{0.85}(CaO)_{0.15}$ solid electrolyte cell deviced for the present study will be briefly described here.

The tube, which was sealed at one end, has a wall width of 2 mm, a diameter of 15 mm and a legth of 40 mm. The bottom portion was coated both inside and outside with a porous platinum film. Platinum electrical leads of 0.5 mm in diameter connect the platinum electrodes of the cell to a potentiometer to measure cell e.m.f. A calibrated thermocouple was also brought into contact with the bottom wall of the cell to measure

the temperature at the bottom portion of the tube. Pure oxygen was circulated the inside of the tube at one atmosphere during the period of measurement.

A galvanic cell may be written at high temperature as follows;

$$Pt,O_2(P_1) \mid \text{solid oxide (stabilized zirconia)} \mid O_2(P_2),Pt$$

The cell e.m.f. is a function of the oxygen partial pressures at the oxygen/Pt electrode, and the maximum electrical energy, 4EF, is given by

$$4EF = -\Delta G = -RT \ln P_1/P_2 \qquad (6)$$

where E is the e.m.f. at a fixed temperature, F, the Faraday constant; P_1, an oxygen partial pressure of a mixed gas at that temperature, and P_2, the reference oxygen pressure, which was kept constant at one atmosphere in the present study. When the cell was inserted into a furnace tube heated to a desired temperature, an oxygen partial pressure in the mixed gas passing through the furnace tube can be readly measured by reading the e.m.f.

In the present study, the oxygen partial pressure obtained by measuring the e.m.f. values according to Eq.(6) was adopted as the actual oxygen partial pressure at any constant temperature.

1-g) Furnace and Temperature Controls ——— A vertical tube-quenching furnace with a 60%Pt-40%Rh wire 0.8mm in diameter winding was used for the equilibrated runs. A brass-made attachment for quenching was connected with the lower end of a mullite furnace tube with 30mm diameter. The mixed gases of one atm. used for controlling the oxygen partial pressure were passed through the furnace from bottom to top.

The furnace temperatures were kept constant to be approximately within ± 2°K by using electric controllers activated by a Pt-13%Rh·Pt thermocouple inserted close to the hot spot of the furnace. The actual temperatures within the furnace were measured by another thermocouple which was calibrated against the melting points of diopside ($CaMgSi_2O_6$), 1391.5°C, and gold (Au), 1063°C.

1-h) Identification of Phases and the Chemical Analysis ——— Phases present in the quenched samples were identified by an X-ray diffraction method using Cu K_α radiation.

The V/O ratio in the starting materials and the quenched samples was determined volumetrically by adopting the Zinc-Amalgam method[29)30)] in order to check the thermogravimetric results.

The Zinc-Amalgam method is as follows; about 100mg of quenched sample was accurately weighed and then heated to dissolve completely with 20ml of pure water and 5-10ml of 18 N H_2SO_4 in a 100ml beaker, while dropping 1 N of potassium

permanganate. The dissolved solution was poured into a reductor. The reductor is illustrated in Fig.1. Air in the reductor was substituted for CO_2 gas and then reductor was shaken for 3-5 minutes. V^{3+} and V^{4+} ions in the solution were completely reduced to V^{2+} ions. The zinc-amalgam was removed from the bottom of the reductor to a lower bottle while substituting the amalgam for a pure water. The titration of V^{2+} ions with standardized 0.1 N potassium permanganate was carried out in the reductor. 0.1 N potassium permanganate directly poured into the reductor from the top as shown in Fig.1. V^{2+} ions were oxidized by permanganate to V^{5+} ions. The amount of vanadium ion was calculated by the amount of the standardized permanganata consumed.

The amount of vanadium was calculated as follows;

$$V\ (mg) = 1.6981 \cdot f \cdot c \tag{7}$$

where f: a factor of 0.1 N $KMnO_4$, c: the amount (ml) of 0.1 N $KMnO_4$ consumed. A certain composition of quenched samples was determined by the following equations;

$$\underset{b}{V} + \underset{(a-b)}{X}(O) = \underset{a}{VO_X} \tag{8}$$

$$X = \frac{M_v}{M_o} \cdot \frac{(a-b)}{b} = 3.184 \cdot \frac{(a-b)}{b} \tag{9}$$

where a is the intial weight (mg) of a dissolved sample, b

Fig.1

reductor for chemical analysis

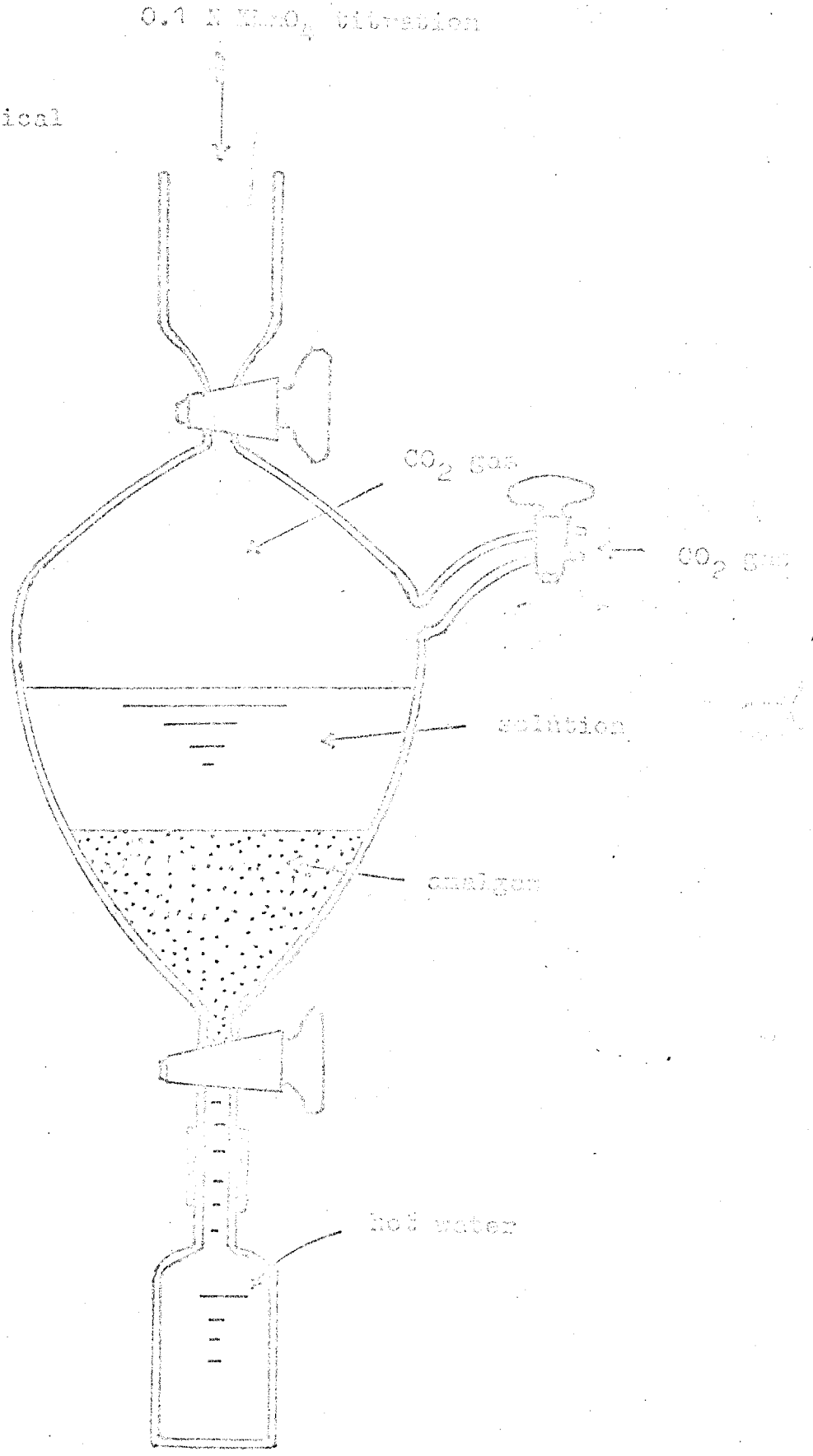

indicates the amount (mg) of vanadium calculated by Eq.(7). M_V and M_O are the atomic weight of vanadium and oxygen, respectively.

1-i) Check of the Equilibrium ——— The rate of approach to the equilibrium state was studied thermogravimetrically. The sample was equilibrated in the gas mixture alternately from a reduced and an oxidized state to ensure that true equilibrium was established. The linear rate of flow of a gas mixture was fixed at about 8mm/sec to 9mm/sec to ensure the equilibrium between gas and solid phases.

1-3 RESULTS AND DISCUSSION

1) Phase Equilibria ——— The equilibrium data including the experimental errors in composition and in oxygen partial pressure at 1400°, 1500°, 1600° and 1700°K are summarized in Table 1.

The V_2O_3, V_3O_5 and V_4O_7 phases were found to be stable under the present conditions. As given in Table 1 and shown in Fig.2, the homogeneity range of the V_2O_3 phase seems to become narrow with decreasing temperature. As decreasing temperature, each phase may be stable at a higher range of oxygen partial pressure. Andersson[5] found a narrow range of homogeneity in the V_3O_5 phase at 900°C, on the other hand, Kosuge et al.[8] estimated fairly wide range of variations in the V/O ratio in the phases V_3O_5 and V_4O_7. In the present study, however, the homogeneity ranges were detected in the V_3O_5 and V_4O_7 phases within the experimental error.

2) Crystal Structure ——— The powder X-ray diffraction patterns of the V_2O_3, V_3O_5 and V_4O_7 phases were identical with those previous investigators[4)6)12)]. The V_2O_3 has a corundom type structure which may be described as a hexagonal close packed array of oxygen atoms with vanadium atoms in two-thirds of the octahedrally coordinated interstices. The α form of Al_2O_3 and Fe_2O_3 (corundom and hematite) and also the oxides Cr_2O_3, Ti_2O_3, V_2O_3, α-Ga_2O_3 and Rh_2O_3 have this type

Table 1 Results of equilibration experiments at 1400°, 1500°, 1600° and 1700°K

1400°K			1500°K		
$-\log Po_2$	CO_2/H_2	Formula VO_x	$-\log Po_2$	CO_2/H_2	Formula VO_x
V_2O_3 phase			V_2O_3 phase		
(± 0.02)		(± 0.002)	(± 0.02)		(± 0.002)
12.8	1	1.500	11.0	1	1.500
11.1	5	1.500	9.89	3	1.500
10.2	10	1.503	9.17	6	1.503
9.47	20	1.508	8.63	11	1.508
8.97	35	1.517	8.41	13	1.510
8.77	44.8	1.523	8.32	15	1.512
8.75	45.3	1.523	8.19	17	1.516
8.68	48.4	1.527) 1.528	8.08	20	1.520
			7.88	25	1.525
			7.65	32	1.534
			7.61	33.4	1.536

(continued)

Table 1

1600°K			1700°K		
- log Po_2	CO_2/H_2	Formula VO_x	- log Po_2	CO_2/H_2	Formula VO_x
(± 0,02)	V_2O_3 phase	(± 0,002)	(± 0,02)	V_2O_3 phase	(± 0,002)
9,85	1	1,500	12,7	0,01	1,500
8,96	2,5	1,501	11,7	0,05	1,500
8,64	3	1,502	11,2	0,01	1,500
8,13	5	1,505	8,84	1	1,500
7,71	8	1,511	8,02	2	1,501
7,51	10	1,515	7,52	3	1,503
7,16	14,5	1,523	6,85	6	1,513
6,87	20	1,535	6,27	11	1,530
6,63	26	1,547	5,87	17	1,551
			5,77	19	1,559
			5,73	20	1,559) 1,560

1400°K			1500°K		
$-\log Po_2$	CO_2/H_2	Formula VO_x	$-\log Po_2$	CO_2/H_2	Formula VO_x
	V_3O_5 phase			V_3O_5 phase	
(± 0.02)		(± 0.002)	(±0.02)		(± 0.002)
8.63	51.2	1.666	7.59	33.7	1.667
8.59	52.9	1.667	7.58	34.2	1.667
8.50	60	1.665	7.56	35	1.666
8.04	100	1.666	6.99	67.3	1.667
7.45	200	1.667	6.53	109	1.667
7.03	300	1.668	6.16	153	1.665
			6.13	156	1.667
	V_4O_7 phase			V_4O_7 phase	
(± 0.03)		(± 0.002)	(±0.03)		(± 0.002)
6.94	333	1.748	6.07	163	1.750
6.91	350	1.748	5.82	200	1.749
6.61	500	1.748	5.46	259	1.751
6.29	700	1.750	5.35	278	1.752
6.18	more oxidized phase		5.32	more oxidized phase	

Table 1 (continued)

1600°K			1700°K		
- log Po_2	CO_2/H_2	Formula VO_x	- log Po_2	CO_2/H_2	Formula VO_x
	V_3O_5 phase			V_3O_5 phase	
(± 0.03)		(± 0.002)	(± 0.04)		(± 0.004)
6.60	26.7	1.666	5.68	21	1.667
6.56	27.8	1.666	5.49	26	1.664
6.49	30	1.665	5.26	34	1.668
6.16	43.1	1.666	4.87	54	1.670
5.73	70	1.666	4.82	57	1.669
5.39	100	1.668	4.76	61	1.671
5.25	114	1.669	4.67	68	1.671
			4.63	71	1.667
			4.59	76	1.671
	V_4O_7 phase			V_4O_7 phase	
(± 0.04)		(± 0.002)	(± 0.05)		(± 0.005)
5.18	120	1.749	4.50	86	1.749
5.13	130	1.750	4.46	91	1.752
4.90	160	1.749	4.37	101	1.752
4.63	200	1.751	4.29	111	1.754
			4.17	131	1.754
			4.12	141	1.755
			4.03	161	1.751
			3.96	181	1.755
4.38	more oxidized phase		3.94	more oxidized phase	

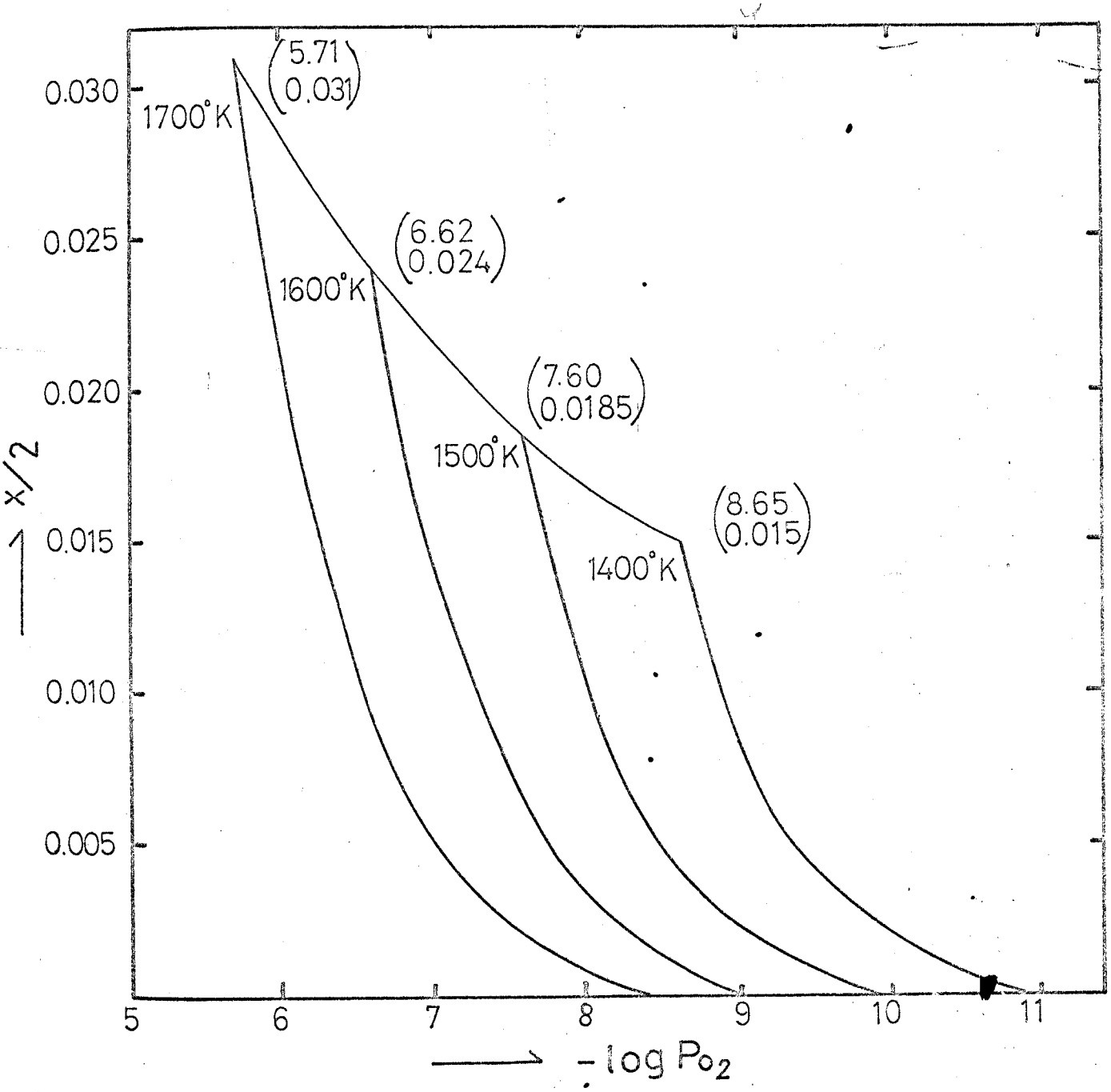

Fig.2 x/2 vs log Po_2 at each temperature. The numbers in parentheses represent the equilibrium oxygen partial pressure and its composition, x/2 in VO_x, in two solid phases eqilibium.

of structure[31]. V_3O_5 has a monoclinic structure ($\alpha=90^\circ$; a, b and c have a different lattice parameter) and the structure of V_4O_7 has not been known. These parameters are summarized in Table 2.

3) The Standard Free Energies of Oxidation and Other Thermodynamic Calculations ——— Among the vanadium oxides on the V_2O_3-VO_2 system, very little is known about the standard free energies of formation of the intermediate compounds, except for both end members, V_2O_3 and VO_2. The standard free energies of formation of V_2O_3 and VO_2 have been compiled by Coughlin[11] and Elliott and Gleiser[19]. They based their calculation on the heats of formation of V_2O_3 and VO_2 from Siemonsen and Ulich's data[32]. Also, the standard free energies of these oxides based on the entropy changes were compiled by Kelley and King[33]. According to Coughlin[11], the free energy equations of following reactions may be written as follows;

$$2V(c) + 3/2\ O_2(g) = V_2O_3(c) \qquad (10)$$

$$\Delta G^\circ(10) = -291350 + 56.49\ T, \quad (600^\circ\text{-}2000^\circ K)\ (cal) \qquad (10')$$

$$2V(c) + 2\ O_2(g) = V_2O_4(c) \qquad (11)$$

$$\Delta G^\circ(11) = -335000 + 73.24\ T, \quad (600^\circ\text{-}1818^\circ K)\ (cal) \qquad (11')$$

Table 2	Crystal Parameter	
Phase		
V_2O_3	rhombohedral	
	$VO_{1.500}$	a = 5.472 Å
		α = 53.80°
V_3O_5	monoclinic	
		a = 9.993 Å
		b = 5.063 Å
		c = 9.872 Å
		β = 138.62°
V_4O_7	unknown	

where T is the absolute temperature.

The standard free energies of oxidation in the following reactions may be calculated on the basis of the equilibrium oxygen partial pressure:

$$VO_{3/2} + 1/12\ O_2 = VO_{5/3} \qquad (12)$$

$$VO_{5/3} + 1/24\ O_2 = VO_{7/4} \qquad (13)$$

Smiltens[34] calculated the standard free energy of oxidation of magnetite (Fe_3O_4) to hematite (Fe_2O_3) by means of Nernst's method[35] at temperatures above 1000°C at which magnetite has an extensive solid solution range. In his paper, he derived a correction term which is related to the formation of a solid solution. The same method was applied to the reaction (12) at 1600°K by Katsura and Hasegawa[12] because of a wide range of homogeneity in the V_2O_3 phase as shown in Fig.2. In the present study, however, the activity of each component in the V_2O_3 phase will be estimated and the free energy of reaction (12) will be calculated on the basis of the activity data.

The solid solution series of V_2O_3 phase may be estimated to be homogeneous mixtures of two components, $VO_{3/2}$ and oxygen (O_2). The activity of oxygen is evaluated to be equal to the partial pressure of oxygen because of a little oxygen content in comparison with the total atmosphere. Thus, for a binary solution, the activity of another component can be calculated

by means of the Gibbs-Duhem equation as follows;

$$\log a_2 = - \int x/2 \, d \log Po_2 \qquad (14)$$

where a_2 is the activity of the $VO_{3/2}$ component, and x is related to the following reaction,

$$VO_{3/2} + x/2 \, O_2 = VO_{3/2 + x} \qquad (15)$$

Po_2 in Eq.(14) indicates an oxygen partial pressure in which a solid solution, $VO_{3/2 + x}$, is equilibrated. The integration was carried out planimetrically at each temperature by using the curves in Fig.2, where x changes from zero to a desired value. The planimetry was duplicated, and the calculated log a_2 is shown in Table 3 together with the error in log a_2.

Since the change in composition of the V_3O_5 phase was stoichiometric within the experimental error, the activity of the $VO_{5/3}$ component may be taken as unity, irrespective of the oxygen partial pressure and the temperature. Thus, for the reaction (12), the equilibrium constant K_1 may be calculated as follows;

$$\log K_1 = \log a_3 - (\log a_2 + 1/12 \log Po_2) \qquad (16)$$

$$= - (\log a_2^* + 1/12 \log Po_2^*) \qquad (16')$$

Here, a_3 means the activity of the $VO_{5/3}$ component, and a_2^* represents the activity of the $VO_{3/2+x}$ component in the V_2O_3 phase which is in equilibrium with the V_3O_5 phase having the stoichiometric composition, Po_2^* means the oxygen partial pressure at which the V_2O_3 phase in equilibrium with the V_3O_5 phase. Values of a_2^* and Po_2^* are logarithmically listed in the last line of Table 3. Calculated values of log K_1 at each temperature are given in Table 4, together with the standard free energy of oxidation of reaction (12), $\Delta G^\circ(12)$.

The standard free energy of oxidation for the reaction (13) can be readily calculated based on the present study, since there was no significant variation in the composition of both V_3O_5 and V_4O_7 phases. Thus the standard free energy of oxidation for reation (13) can be found by the van't Hoff equation;

$$\Delta G^\circ = nRT \ln Po_2(eq) \qquad (17)$$

where n is the number of moles in an equation, and where $Po_2(eq)$ is the equilibrium oxygen partial pressure at which two solid phases are in equilibrium. Calculated values of the standard free energy of oxidation for reation (13) at each temperature are given in Table 4 together with values of Po_2^{**} at which both V_3O_5 and V_4O_7 phases are in equilibrium. The present values of both $\Delta G^\circ(12)$ and $\Delta G^\circ(13)$ at 1600°K are silghtly higher than those previously obtained by Katsura and Hasegawa[12]

Table 3 Relationship between composition and activities of oxygen (Po_2), $VO_{3/2+x}$ (a_2), in the V_2O_3 phase at temperatures 1400°, 1500°, 1600° and 1700°K on the basis of reaction (15) and (16) using Fig. 2.

composition x/2	1700°K		1600°K		1500°K		1400°K	
	$-\log Po_2$	$-\log a_2$ $\times 10^{-2}$	$-\log Po_2$	$-\log a_2$ $\times 10^{-2}$	$-\log Po_2$	$-\log a_2$ $\times 10^{-2}$	$-\log Po_2$	$-\log a_2$ $\times 10^{-2}$
0.005	7.02 (±0.02)	0.22 (±0.02)	7.76 (±0.02)	0.24 (±0.02)	8.46 (±0.03)	0.24 (±0.03)	9.31 (±0.04)	0.27 (±0.03)
0.010	6.55 (±0.02)	0.56 (±0.03)	7,27 (±0.02)	0.59 (±0.03)	8.05 (±0.03)	0.54 (±0.03)	8.85 (±0.03)	0.60 (±0.04)
0.015	6.27 (±0.02)	0.91 (±0.03)	6.95 (±0.02)	0.93 (±0.03)	7.75 (±0.03)	0.91 (±0.04)	8.65 (±0.04)	0.87 (±0.04)
0.0185	-	-	-	-	7.60 (±0.03)	1.16 (±0.04)	-	-
0.020	6.07 (±0.02)	1.26 (±0.03)	6.76 (±0.02)	1.33 (±0.03)	-	-	-	-
0.024	-	-	6.62 (±0.04)	1,64 (±0.04)	-	-	-	-
0.025	5.88 (±0.02)	1,68 (±0.03)	-	-	-	-	-	-
0.031	5.71 (±0.05)	2,16 (±0.04)	-	-	-	-	-	-

Table 4 Caluculated values of some thermodynamic data corresponding to reactions (1) and (2) at each temperature.

Temperature ^{o}K	log K_1	$-\Delta G^{o}(2)$ cal	log Po_2^{**}	$-\Delta G^{o}(2)$ cal
1400	0.730 ± 0.004	4680 ± 40	6.99 ± 0.08	1870 ± 30
1500	0.645 ± 0.003	4430 ± 30	6.10 ± 0.06	1740 ± 30
1600	0.568 ± 0.004	4160 ± 40	5.22 ± 0.07	1590 ± 40
1700	0.497 ± 0.005	3870 ± 50	4.55 ± 0.10	1470 ± 40

$\Delta H^{o}(1)$ = - 8470 ± 230 cal $\quad$ $\Delta H^{o}(2)$ = - 3720 ± 250 cal

$\Delta S^{o}(1)$ = - 2.70 ± 0.30 e.u. $\quad$ $\Delta S^{o}(2)$ = - 1.44 ± 0.13 e.u.

and the present values may be more reliable because of a higher accuracy of the present experiment.

As shown in Fig.3, the value of log K_1 seems to be proportional to the reciprocal of the absolute temperature, 1/T, within the experimental errors, then the slope gives the following value,

$$\frac{d \log K_1}{d\,(1/T)} = - \frac{\Delta H^{\circ}(12)}{2.303\ R} = - (\ 1.85 \pm 0.05\ ) \cdot 10^3 \qquad (18)$$

where $\Delta H^{\circ}(12)$ and R are the heat of reaction (12) and the gas constant, respectively. The heat of reaction (13) is also calculated similarly from the slope in Fig.4 which gives the constant value of $24 \cdot (\ \Delta H^{\circ}(13)/2.303\ R\ )$. Calculated values of the heat of reaction (12) and (13) based on the least square method are given in Table 4.

The enthalpies of reaction (12) and (13) are constant over the present temperature range. The standard free energies of oxidation of the same reactions seem to be proportional to temperature. The relations are illustrated in Fig.5. The standard entropy changes, ΔS°, of reaction (12) and (13) are found from the slope of the line by the least square method as seen in Fig.5. Values of the entropy are also given in Table 4 over the temperature interval from 1400° to 1700°K. As shown in Fig.4 and Fig.5, the slopes hold a constant value

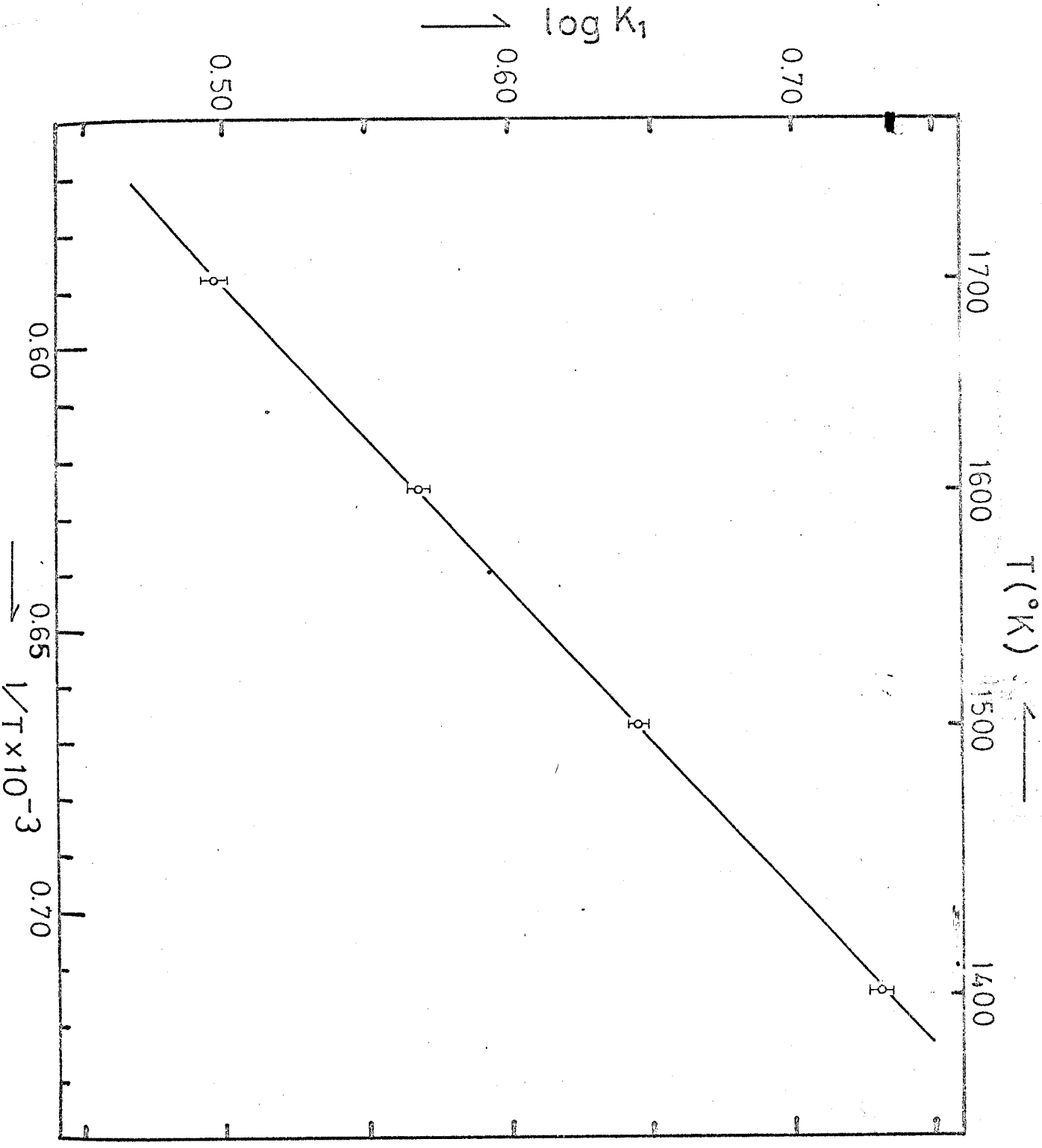

Fig.3 Relationship between log K_1 and reciprocal absolute temperature.

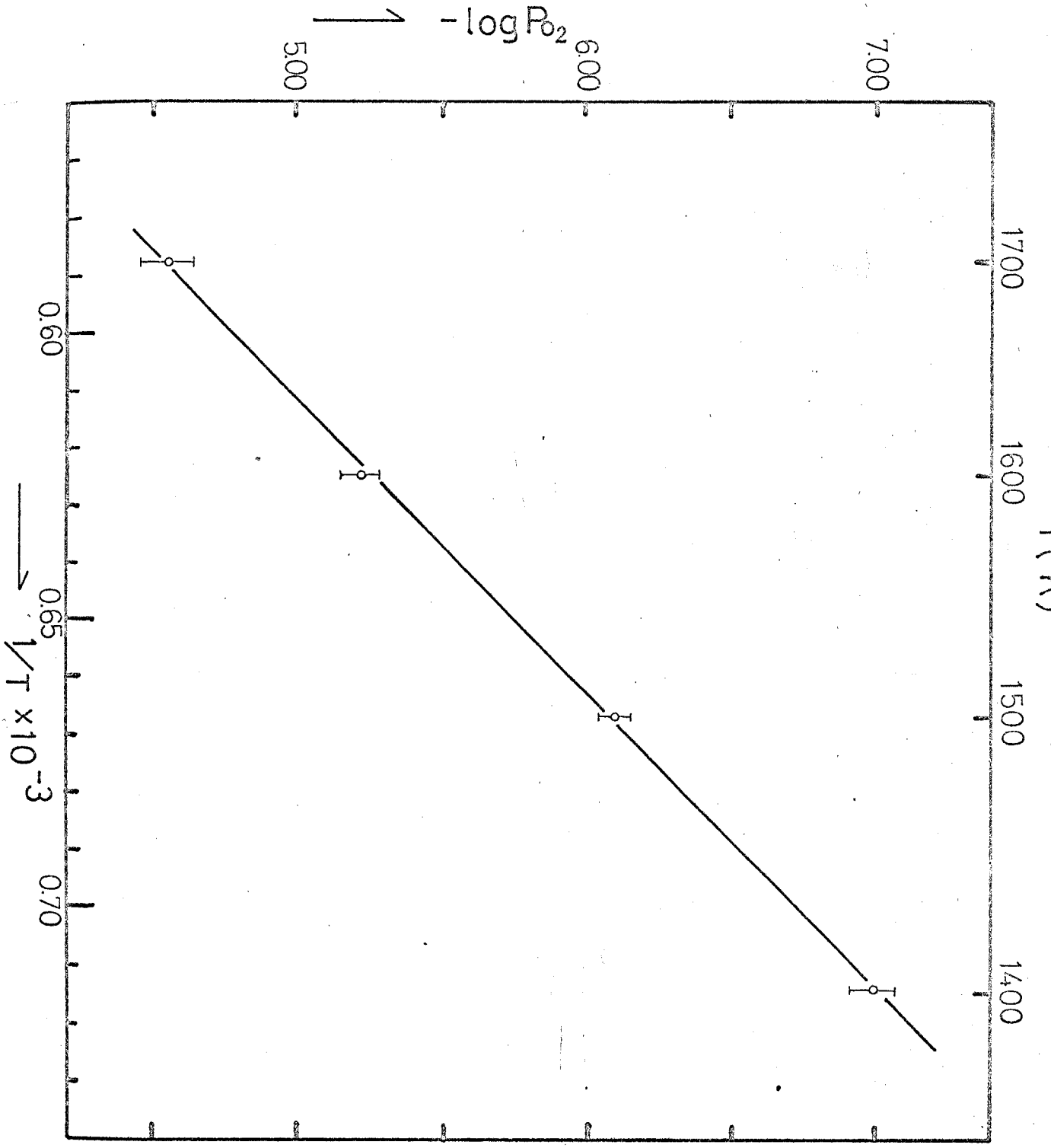

Fig.4 Equilibrium oxygen partial pressure corresponding to the reaction (13) vs 1/T.

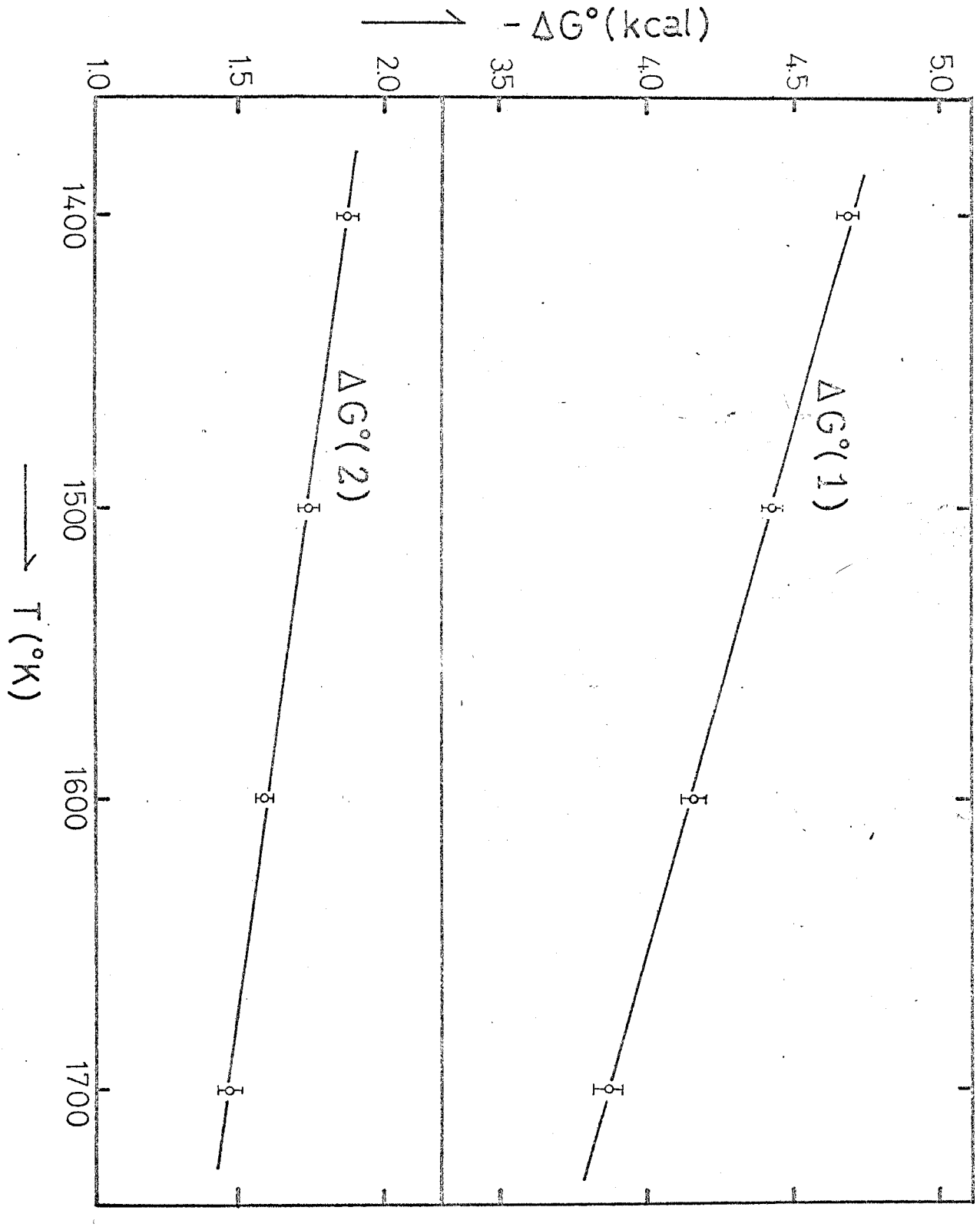

Fig.5 Relationship between the standard free energy and temperature.

in the range of temperatures from 1400° to 1700°K. Hence, values of ΔH° and ΔS° may be kept constant over the temperature range from 1400° to 1700°K.

1-4) Summary ——— Phase equilibria in the V_2O_3-V_4O_7 system were studied at 1400°, 1500°, 1600° and 1700°K by varying the oxygen partial pressure. Besides the three phases of V_2O_3, V_3O_5 and V_4O_7 were stable in this system, the vanadium sesquioxide has an extensive range of solid solution at the above mentioned temperatures. The standard free energies of oxidation of both V_2O_3 to V_3O_5 and V_3O_5 to V_4O_7 were precisely determined on the basis of the equilibrium oxygen partial pressure at each above temperature. The standard enthalpy and the entropy changes of these reactions were also calculated from the free energy data.

CHAPTER 2

Phase equilibria in the System $FeO-Fe_2O_3-V_2O_3$ at 1500°K

2-1 INTRODUCTION

The system Fe-V-O has attracted a great deal of interest among metallurgists as well as ceramists and geochemists. Accurate phase equilibria, however, have not been presented, particularly at high temperature. Separate studies on the Fe-O and V-O systems were carried out by Darken and Gurry[18] and many other investigators as described in Chapter 1. Vanadium is a minor element in the earth's crust, and the average content is ordinary mentioned to be 0.02 per cent in igneous rocks. The most common mineral containing vanadium in igneous rocks is the member of the Fe_3O_4 (magnetite) - FeV_2O_4 solid solution series, and also the solid solution series are expected of interesting magnetic properties.

Burdese[13] studied phase equilibria on the Fe-V-O system and synthesized FeV_2O_6, FeV_2O_4 and $FeVO_4$. Rahmel et al.[36] first summarized the phase equilibria at the temperature range from 550° to 1000°C. Vorob'ev et al.[37] studied the Fe_3O_4-FeV_2O_4 and wustite solid solutions at 1000°K. Kunnmann et al.[38] synthesized some transition metal oxides containing FeV_2O_4 and Fe_2VO_4 by varying oxygen partial pressures at the temperature

from 1073° to 1380°K and calculated the standard free energy of FeV_2O_4. Recently, Schmahl and Dillenbrug[39] studied the phase equilibria on the Fe-V-O system at 900°C and calculated activity for FeV_2O_4-Fe_3O_4 solid solution series and the standard free energy of FeV_2O_4. Also, they recognized that Fe_2O_3-V_2O_3 solid solution has an immiscible region in the range 78-93 mole per cent V_2O_3 at 900°C. In the solid solution series, Cox et al.[40] similarly found the immiscibility gap in the range 80-90 mole per cent V_2O_3 by their magnetic data at 1000°C.

In the present study, accurate phase equilibria FeO-Fe_2O_3-V_2O_3 system at 1500°K will be studied by varying the oxygen partial pressure and the standard free energies of some reactions which are reasonable in this system will be calculated on the basis of the equilibrium oxygen partial pressure. Also, activities of the FeV_2O_4-Fe_3O_4 solid solution series will be evaluated by using the activity data of wustite phase, which were calculated by Darken and Gurry[18] and the oxygen partial pressure data of this study, which were in equilibrium with metallic iron.

2-2 EXPERIMENTAL

2-a) General Procedure ——— Two different experimental methods were used in the present study; quenching and thermogravimetry.

In the quenching method, oxide samples were heated at 1500°K and at a chosen oxygen partial pressure until equilibrium was attained among gas and condensed phases. Total compositions were determined by means of the gravimetric weight gain method.

In the thermogravimetirc method, a pellet of oxide mixtures was suspended in a vertical tube furnace by a thin platinum wire from the bottom of quick weighing valance. The weight changes were recorded as a function of oxygen partial pressure at 1500°K. The data thus obtained reflect changes in phase assembledges and serve to supplement the observations made by the quenching technique.

2-b) Materials ——— V_2O_5 was obtained by decomposition of reagent grade of ammonium meta vanadate in air at 450°C for 12 hr. Analytical-grade Fe_2O_3 was heated in air at 700°C for 12 hr. Mixtures of desired ratio of the two oxides were then prepared. The mixture was loosely pressed into a small-size platinum crucible, and heated at 650°C in an atmosphere of a mixed gas of CO_2/H_2 = 1 for 20 minutes. An error in the atomic ratio of V/Fe in a mixture was estimated to be within

± 0.1 per cent. The prepared sample was a mixture of reduced forms of vanadium and iron oxides. The grinding, pressing and heating were repeated to obtain an uniform mixture. The mixed oxide sample was removed from the crucible and suspended in a furnace tube; here it was heated for 10-18 hr at 1500°K in a desired ratio of CO_2/H_2 until equilibrium was attained between the gas and the solid phases. The detailed techniques are the same as those described in Chapter 1, 1-2.

2-c) Analysis of Total Compositions ——— Total compositions of the quenched sample were determined by the gravimetric weight gain method. The sample was completely oxidized to a mixture of V_2O_5 and Fe_2O_3 at 800°C in air for 24-48 hr, and then was weighed. As the Fe_2O_3/V_2O_5 mol ratio of starting material is known, total compositions of the quenched sample are evaluated by the weight difference before and after the oxidation as following equations;

$$x = \frac{a}{w_1 - w_2/2} - \frac{b(w_2 r + w_3)}{(w_2 r + w_4)(w_1 - w_2/2)} \qquad (19)$$

$$y = \frac{a}{w_1 - w_2/2} - \frac{1}{2}\left[\frac{a}{w_1 - w_2/2} - \frac{b(w_2 r + w_3)}{(w_2 r + w_4)(w_1 - w_2/2)}\right] \qquad (20)$$

$$z = \frac{b}{w_2 r + w_4} \qquad (21)$$

where x, y and z correspond to mol ratio of FeO, Fe_2O_3 and V_2O_3, respectively. a indicates the initial weight of a quenched sample and b represents the weight of completely oxidized sesquioxide mixture, and r shows atom ratio, Fe/V, of an initial mixture of Fe_2O_3 and V_2O_5. w_1, w_2, w_3 and w_4 correspond to formula weights of FeO, Fe_2O_3, V_2O_3 and V_2O_5, respectively. The vaporization of V_2O_5 was insignificant during heating within the present accuracy. The error of total compositions was estimated to be within ± 0.2 per cent.

2-d) Control of Atmosphere ——— A desired partial pressure of oxygen was provided by using a gas mixture of CO_2 and H_2 or CO_2 and O_2 and it was calibrated by the solid electrolyte cell composed of stabilized zircornia. Their procedures are just the same as those described in Chapter 1, 1-2.

2-e) Thermogravimetry ——— The rate of approach to equilibrium was studied thermogravimetrically. Also, the method was used to determine ranges of oxygen partial pressure and composition in which spinel solid solution exists in equilibrium. In this method, the starting materials were prepared as follows; a mixture in a desired ratio of Fe_2O_3/V_2O_5 was heated at 650°C in a mixed gas of CO_2/H_2 =1 for 20 minutes. The prepared sample was ground and was loosely pressed into a small-size platinum crucible and then heated at 1500°K in an atmosphere, CO_2/H_2 = 1, for 5 minutes. The sintered sample was

then pulled up from the top of the furnace. The procedure was repeated to make into a sinter completely. The prepared pellet of about 2g was removed from the crucible and made some holes to attain the sample easily to an equilibrium. The pellet was suspended into a tube of furnace and measured the weight change by varying the oxygen partial pressure. A boundary of spinel and any other phases was decided by a rapid weight changes with the variation of oxygen partial pressure. The error of vaporization was corrected by measuring weights between at any oxygen partial pressure and at a starting oxygen partial pressure.

The range of defect in the spinel solid solution series was determined by measuring the weight changes according to the following equations;

$$\underset{a}{(Fe_mV_n)_3O_4} + \underset{(b-a)}{x/2\ O_2} = \underset{b}{(Fe_mV_n)_3O_4} + x \qquad (22)$$

$$x = \frac{3(mM_{Fe} + nM_V) + 4M_O}{M_O} \cdot \frac{(b-a)}{a} \qquad (23)$$

$$(m + n = 1)$$

where a represents the weight of stoichiometric spinel and b indicates the weight at a certain equilibrated oxygen partial pressure. m and n are atom fractions of iron and vanadium. M_{Fe}, M_V and M_O indicate atomic weights of iron, vanadium and

oxygen, respectively.

2-f) Identification of Phases ——— The phases present in quenched samples were identified by an X-ray diffraction method using Fe K_α radiation.

The presence of metallic iron in the phase assemblages was evidenced by the liberation of hydrogen gas when samples were dipped in hydrochloric acid. This test is sensitive enough to detect iron in amounts as small as 0.2 per cent in a previous study[17].

2-3 RESULTS AND DISCUSSION

1) Phase Equilibria ——— Equilibrium data obtained at 1500°K are summarized in Table 5 and illustrated graphically in Fig.6.

Three oxide phases have stable existence under the present experimental conditions: Sesquioxide solid solution, spinel solid solution and wustite solid solution.

Compositions of sesquioxide are well represented by the formula $(Fe \cdot V)_2O_3$. A deviation of oxygen to cation ratio below the stoichiometric 3:2 was not found within the experimental error. Sesquioxides of 80-100 mol per cent Fe_2O_3 were by using a gas mixture of CO_2 and O_2. Each phase of sesquioxide solid solution was identified by X-ray diffraction method.

The spinel phase is a ternary solid solution having stable existence at 1500°K within the composition area Fe_3O_4-FeV_2O_4-Fe_2O_3. The area of the spinel solid solution at 1500°K in the FeO-Fe_2O_3-V_2O_3 system is given together with isobaric lines of the oxygen partial pressure in Fig.7. The figure illustrates the relationship between atomic ratio of 4(Fe + V)/O and comsitional parameter x for the general formula of the spinel $Fe_{1+2x}V_{2-2x}O_4$ ($0 \leqq x \leqq 1$). The variation of 4(Fe + V)/O, which is a measure of defect structure of the present spinel, is seen to depend on the value of x and the amount of defect metal from stoichiometric increases as the iron content of the phase increases. For exsample, the spinel with x = 0.5 varied

Table 5 Results of equilibration experiments at 1500°K at various oxygen partial pressures

mol % x: FeO y: Fe_2O_3 z: V_2O_3

ses. : sesquioxide solid solution

sp. : spinel solid solution

wu. : wustite solid solution

- log Po_2 ± 0.05	x	y	z	phases present
13.13	50.3	0	49.7	ses + sp
11.71	9.8	4.5	85.7	ses + sp
	27.1	3.7	69.2	ses + sp
	41.2	3.2	55.6	ses + sp
	45.8	2.8	51.4	ses + sp
11.61	49.6	16.5	33.8	sp
	57.9	13.7	28.4	sp + wu
11.48	51.1	19.1	29.8	sp + wu
	66.0	13.9	20.1	sp + wu
	72.7	11.4	15.9	sp + wu
	78.4	9.4	12.2	sp + wu
	84.0	7.2	8.7	sp + wu
	88.7	5.8	5.6	wu
	92.0	5.3	2.7	wu
11.36	50.2	19.8	30.0	sp + wu
	59.4	17.1	23.4	sp + wu
	63.8	15.8	20.4	sp + wu
	70.8	13.0	16.2	sp + wu
	76.9	10.8	12.3	sp + wu
	82.5	8.7	8.8	sp + wu
	87.4	6.9	5.6	sp + wu
	91.5	5.8	2.7	wu

Table 5 (continued)

$-\log Po_2$ ± 0.05	x	y	z	phases present
10.94	5.3	6.9	16.2	ses + sp
	24.7	5.3	70.0	ses + sp
	39.4	4.3	56.3	ses + sp
	44.4	3.8	51.8	ses + sp
	48.6	4.1	47.3	ses + sp
	48.8	5.9	45.4	sp
	49.7	20.3	30.0	sp
	52.6	22.9	24.5	sp + wu
	57.9	20.8	21.3	sp + wu
	65.3	17.8	16.9	sp + wu
	73.0	14.3	12.7	sp + wu
	79.2	11.8	9.1	sp + wu
	85.4	8.9	5.7	sp + wu
	90.1	7.1	2.8	wu
	93.5	6.5	0	wu
10.04	50.3	30.9	18.7	sp + wu
	61.5	24.7	13.8	sp + wu
	71.0	19.4	9.6	sp + wu
	78.7	15.3	6.0	sp + wu
	82.2	13.4	4.4	sp + wu
	85.5	11.6	2.8	wu
	89.3	10.7	0	wu
9.75	49.5	35.4	15.1	sp
	61.4	28.2	10.4	sp + wu
	71.9	21.8	6.4	sp + wu
	81.4	15.6	3.0	sp + wu

Table 5 (continued)

$-\log Po_2$ ± 0.05	x	y	z	phases present
9.01	49.6	40.9	9.4	sp
	49.6	42.8	7.5	sp
	49.7	44.7	5.6	sp
	61.4	35.1	3.5	sp + wu
	82.6	17.4	0	wu
8.59	0	20.0	80.0	ses
	12.1	17.4	70.4	ses + sp
	23.4	14.8	61.8	ses + sp
	30.1	13.3	56.6	ses + sp
	41.9	10.6	47.5	ses + sp
	48.9	13.3	37.8	sp
	49.2	16.9	34.0	sp
	49.5	35.4	15.0	sp
	49.3	43.2	7.5	sp
	49.5	46.7	3.8	sp
7.61	2.0	28.8	69.3	ses + sp
	13.4	24.4	62.1	ses + sp
	29.4	19.5	51.1	ses + sp
	39.1	16.6	44.3	ses + sp
6.30	11.6	36.6	51.8	ses + sp
	25.7	30.7	43.6	ses + sp
	35.9	27.2	37.0	ses + sp
	46.9	22.5	30.6	sp
	47.0	30.0	23.0	sp
4.41	3.0	52.6	44.4	ses + sp
	20.2	43.9	36.0	ses + sp
	35.1	37.4	27.5	ses + sp
	42.2	34.2	23.6	ses + sp

Table 5 (continued)

$-\log Po_2$ ± 0.05	x	y	z	phases present
2.94	8.8	72.1	19.1	ses + sp
	24.7	62.2	13.1	ses + sp
	39.7	52.4	8.0	ses + sp

Fig 6. Phase Equilibria of V_2O_3-Fe_2O_3-FeO at 1500°K

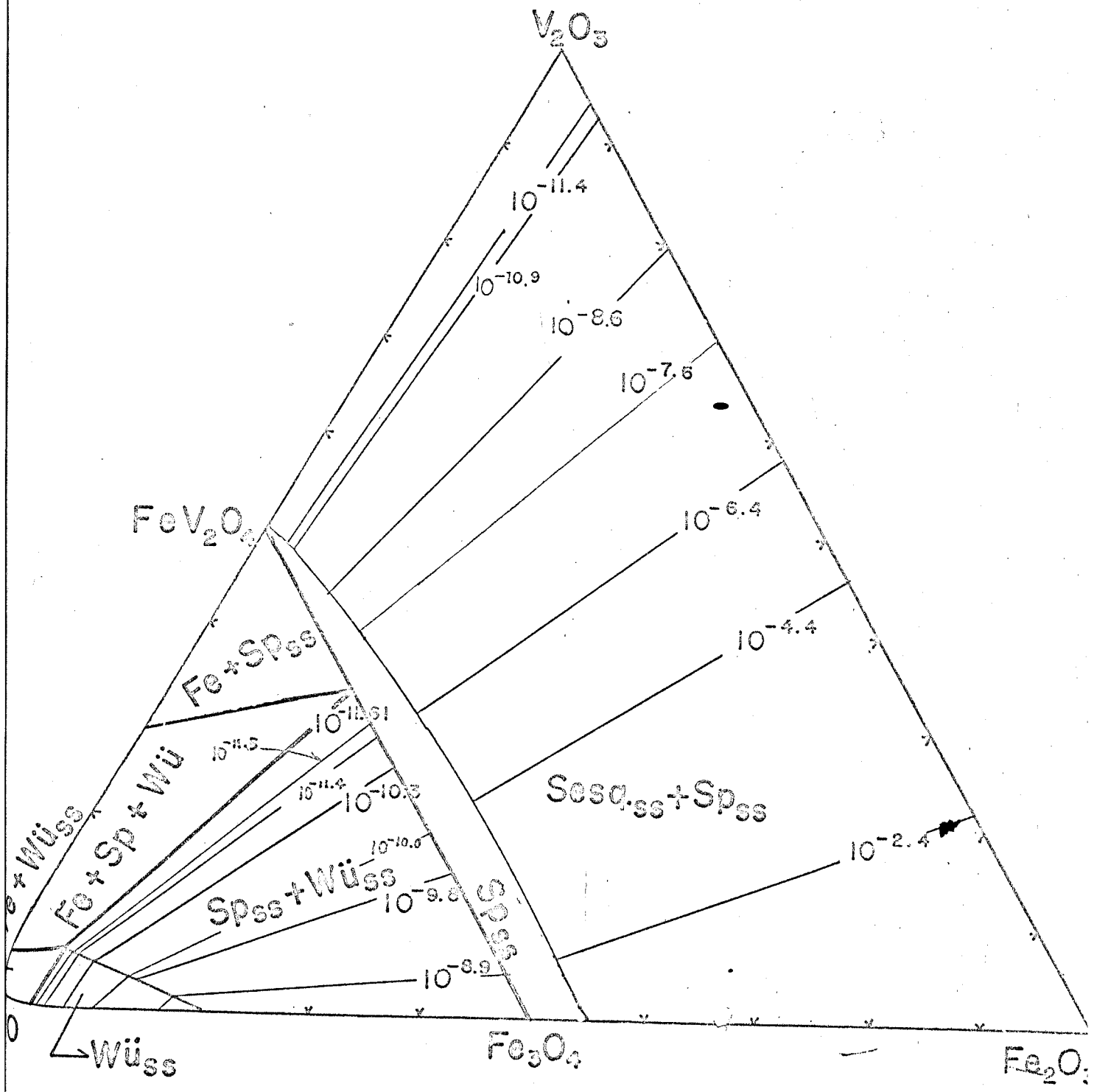

its composition from $(Fe_{2/3}V_{1/3})_3O_4$ to $(Fe_{2/3}V_{1/3})_{2.965}O_4$, while the spinel FeV_2O_4 was stoichiometric within the experimental error. According to the data of Darken and Gurry[18], magnetite (Fe_3O_4) changes its composition from stoichiometric to $Fe_{2.956}O_4$. As seen in Fig. 7, extrapolating the boundary curve in the present study consisted with their data within the experimental error. The relationship between the region of oxygen partial pressure and composition parameter x in which the spinel phase exists in equilibrium is shown in Fig.8. In Fig.7, isobaric lines of oxygen were concentrated near the stoichiometric spinel solid solution when the partial pressure of oxygen became lower, and a spinel with a stoichiometric composition was decomposed to more reduced phases which are either metallic iron or vanadowustite. The spinel with a greater metal to oxygen ratio than 3/4 was not found in the present study. These situations are quite similar to the case of the spinel solid solutions, Fe_2TiO_4-Fe_3O_4[41] and $FeCr_2O_4$-Fe_3O_4[16].

The wustite phase is characterized by wide variation in Fe/O as well as the presence of some V^{3+} ions in the structure. The extent of these compositional variations is seen from Fig.6. Difficulties were encountered in quenching of wustite phase. Therefore, total compositions of this phase contain somewhat larger error than those of other phases.

The results in the present study at 1500°K on the binary system FeO-Fe_2O_3 consisted with those obtained by Darken and

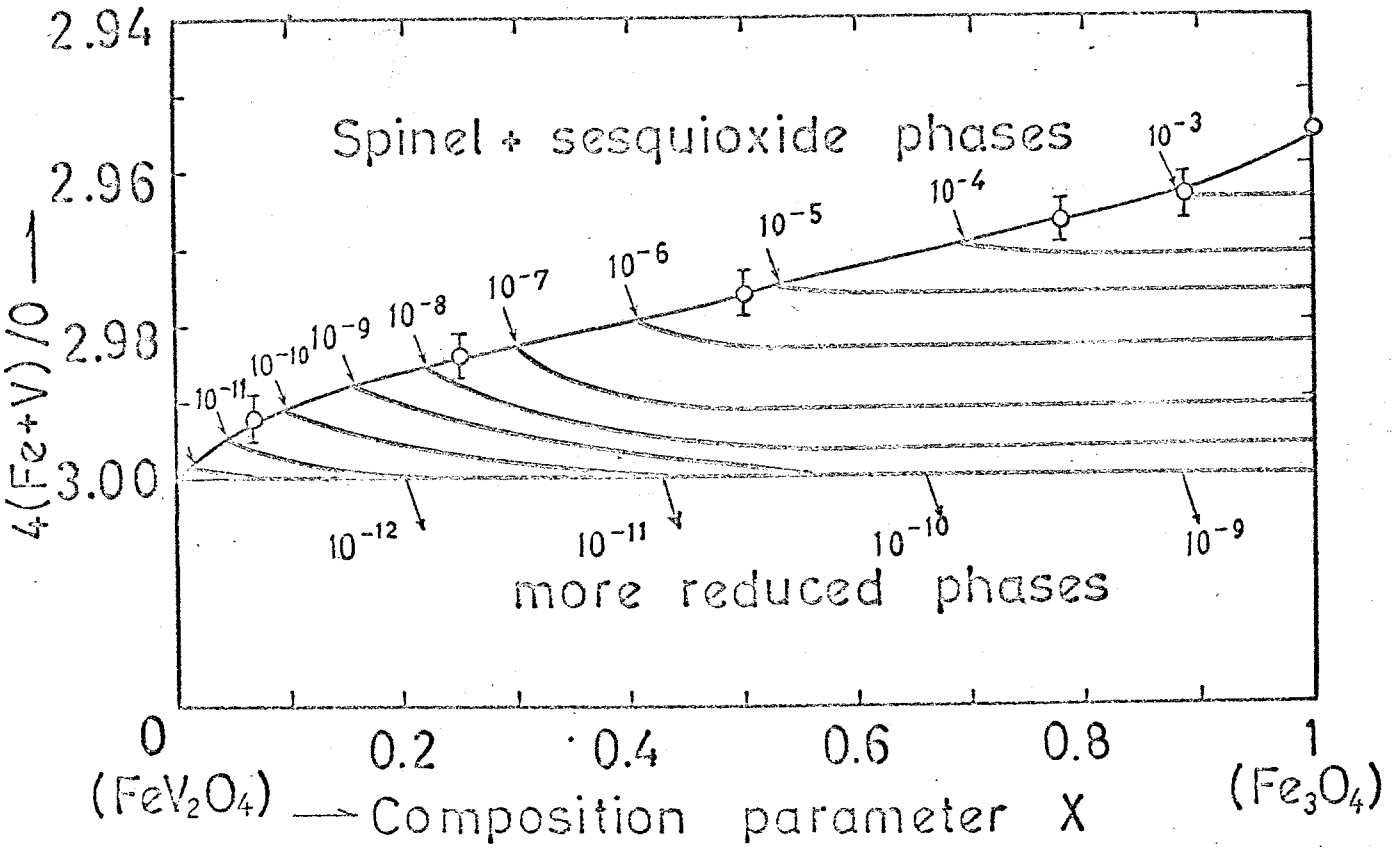

Fig.7 Area of the spinel solid solution concerning with composition parameter x for the $Fe_{1+2x}V_{2-2x}O_4$ ($0 \leqq x \leqq 1$) at 1500°K. Some curved lines in the area indicate the isobaric lines of oxygen partial pressure.

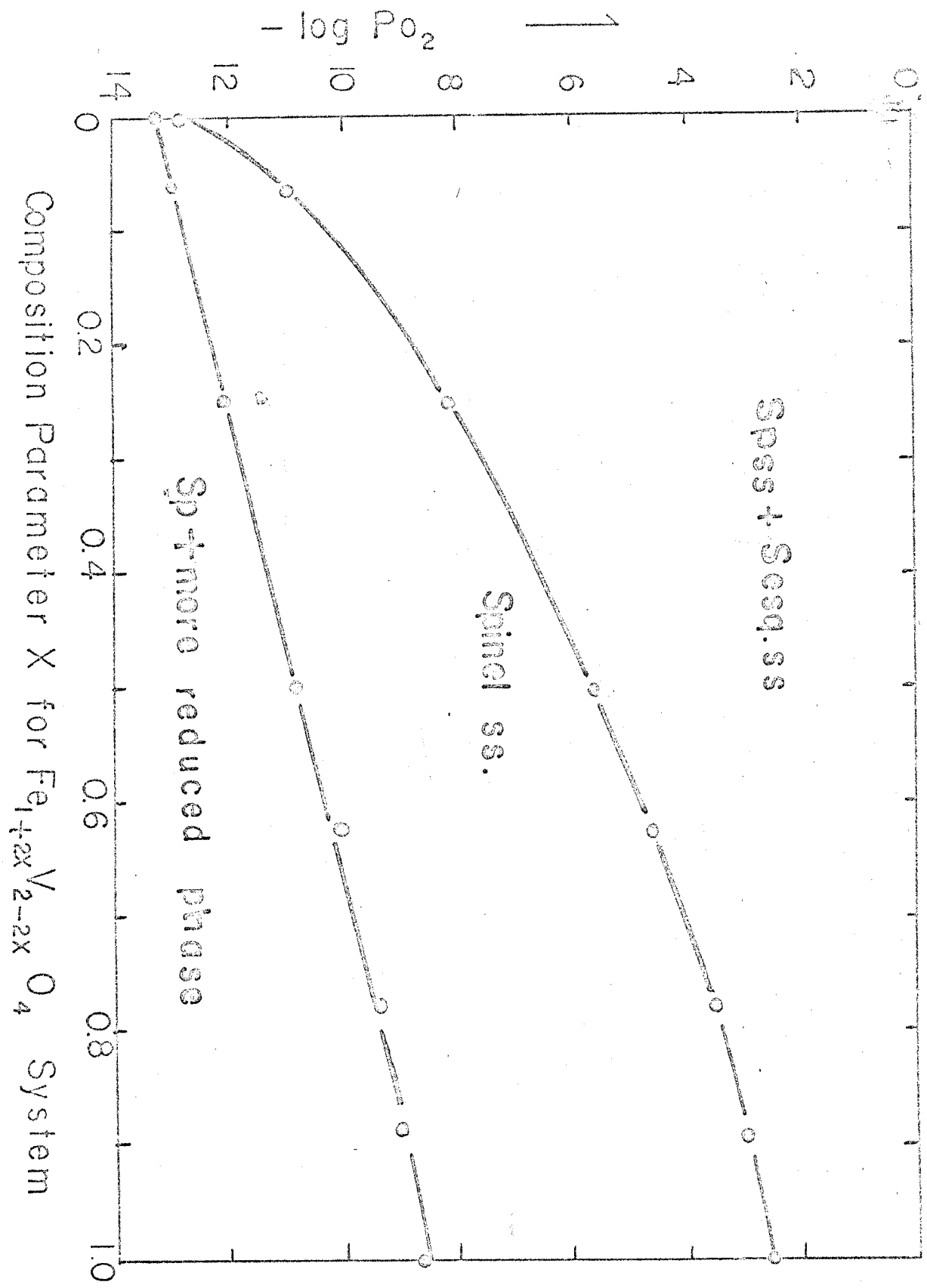

Fig.8 Relationship between equilibrium oxygen partial pressure and composition parameter x for $Fe_{1+2x}V_{2-2x}O_4$ under which the spinel solid solurion exists in equilibrium.

Gurry[18] within the experimental error. Therefore, their data also were used on the binary system.

The sesquioxide phase with rhombohedral (corundom-type) structure extends as a continuous solid solution series between the end members Fe_2O_3 and V_2O_3. On the other hand, Schmahl and Dillenburg[39] and Cox et al.[40] reported the immiscible gap in the range 80 to 90 mole per cent V_2O_3 at 900°C and 1000°C, respectively. The immiscible gap, however, was not found in the present study throughout the Fe_2O_3-V_2O_3 system at 1500°K within the experimental error.

The phase equilibria FeO-Fe_2O_3-V_2O_3 system were similar to those of FeO-Fe_2O_3-Cr_2O_3 system[16]. Some characteristic differences were following that deviation of oxygen to cation ratio below the stoichiometric 3:2 in the sesquioxide phase was not found in the present investigation, and the spinel phase region in equilibrium with mettalic iron (almost from FeV_2O_4 to Fe_2VO_4) in this study was larger than those of magnetite-iron chromite solid solution series[16]. The latter may be partly due to the difference of experimental temperature between the present and previous[16] studies.

2) Thermodynamic Calculations ——— In addition to the data above, the oxygen pressure at which metallic iron, FeV_2O_4 and sesquioxide coexist in equilibrium was determined in this investigation ($\log Po_2 = -13.25 \pm 0.05$). This value was obtained thermogravimetrically as shown in Fig.8. Therefore,

the standard free energy of formation of FeV_2O_4 from metallic iron and sesquioxide components at 1500°K can be calculated as follows;

$$Fe + V_2O_3 + 1/2\ O_2 = FeV_2O_4 \qquad (A)$$

and the standard free energy for reaction (A) is given by following equations;

$$\Delta G^\circ(A) = -RT \ln \frac{a_{FeV_2O_4}}{a_{Fe} \cdot a_{V_2O_3} \cdot Po_2^{1/2}} = 2.303/2\ RT \log Po_2 \qquad (A')$$

$$= -45500 \pm 200 \text{ cal}$$

where a_{Fe}, $a_{V_2O_3}$ [42] and $a_{FeV_2O_4}$ represent the unit activity because of pure components in this oxygen partial pressure, $\log Po_2(A) = -13.25$.

The standard free energy of reaction (A) was reported by Kunnmann et al.[38] at a temperature range from 1073° to 1380°K by varying the oxygen partial pressure using CO_2/CO gas mixtures. The standard free energy resulted from the present study was reasonably consisted with extrapolated value at 1500°K based on the data by Kunnmann et al[38]. According to the data of Darken and Gurry[18], the oxygen partial pressure in which metallic iron and wustite phases were in equilibrium was estimated logarithmically to be $\log Po_2 = -11.58 \pm 0.05$

at 1500°K. Therefore, the standard free energy of formation of wustite from metallic iron can be readily calculated;

$$0.95\ Fe + 1/2\ O_2 = Fe_{0.95}O \qquad (B)$$

and the standard free energy of reaction (B) is calculated as follows;

$$\Delta G^\circ(B) = - RT \ln \frac{a_{Fe_{0.95}O}}{a_{Fe}^{0.95} \cdot Po_2^{1/2}} = 2.303\ RT/2 \log Po_2(B) \qquad (B')$$

$$= - 39700 \pm 200 \quad cal$$

where $\log Po_2(B) = - 11.58 \pm 0.05$, and activities a_{Fe} and $a_{Fe_{0.95}O}$ are unit.

Subtraction of Eq.(B) from Eq.(A) gives the following equation;

$$0.05\ Fe + V_2O_3 + Fe_{0.95}O = FeV_2O_4 \qquad (C)$$

and the standard free energy of reaction (C) is given by

$$\Delta G^\circ(C) = \Delta G^\circ(A) - \Delta G^\circ(B) = RT \ln \frac{Po_2(A)}{Po_2(B)} \qquad (C')$$

$$= - 5800 \pm 400 \quad cal$$

Activities of magnetite in stoichiometric FeV_2O_4-Fe_3O_4 spinel solid solution series may be calculated by using the activities of wustite solid solution, which was evaluated by Darken and Gurry[18] and the oxygen partial pressures coexisting metallic iron and wustite ($Fe_{0.95}O$), and wustite ($Fe_{0.855}O$) and stoichiometric magnetite phases, respectively.

The standard free energy of formation of "$Fe_{0.954}O$", $\Delta G^\circ(B)$, at 1500°K was just described above in Eq.(B'). According to the data of Darken and Gurry[18], the compositional range of wustite solid solution changes from "$Fe_{0.954}O$" to "$Fe_{0.855}O$" and the logarithmic activity varies from 0 to 0.156 at 1500°K, respectively. Therefore, the standard free energy of formation of wustite solid solution at 1500°K, $\Delta G^\circ_{ss}(D)$, may be calculated as follows;

$$\Delta G^\circ_{ss}(D) = RT \ln a_{"Fe_{0.855}O"} = -1070 \pm 10 \quad cal \qquad (D)$$

The stoichiometric magnetite coexists with wustite phase in equilibrium at the oxygen partial pressure, $\log Po_2 = -8.73$, as shown in Fig.8. Thus, the standard free energy of following equation can be evaluated;

$$3\ "Fe_{0.855}O" + 1/2\ O_2 = Fe_3O_4 \qquad (E)$$

$$\Delta G^\circ(E) = -2.303\ RT \log \frac{a_{Fe_3O_4}}{a_{"Fe_{0.855}O"}{}^3 \cdot Po_2{}^{1/2}} \qquad (E')$$

$$= -30000 \pm 200 \quad cal$$

where $a_{Fe_3O_4}$ is unit, and log Po_2 = - 8.73, log $a_{"Fe_{0.855}O"}$ = - 0.156, respectively.

The reaction corresponding to the formation of stoichiometric magnetite may be written;

$$3\ Fe + 2\ O_2 = Fe_3O_4 \qquad (F)$$

The standard free energy of Eq.(F), $\Delta G^\circ(F)$, may be equal to the following equation and evaluated by substituting actual values for respective ΔG°;

$$\Delta G^\circ(F) = 3\ \Delta G^\circ(B) + 3\ \Delta G^\circ_{ss}(D) + \Delta G^\circ(E)$$

$$= - 152430 \pm 830 \text{ cal} \qquad (F')$$

Then, the standard free energy and the equilibrium constant, K_G of following reaction can be calculated as follows;

$$3\ "Fe_{0.954}O" + 1/2\ O_2 \overset{K_G}{=} Fe_3O_4 \qquad (G)$$

$$\Delta G^\circ(G) = \Delta G^\circ(F) - 3\ \Delta G^\circ(B)$$

$$= - 33210 \pm 1430 \text{ cal}$$

$$= - RT \ln K_G \qquad (G')$$

$$\log K_G = 4.84 \pm 0.22$$

The general equation for the oxidation of wustite phase is given by;

$$3\ \text{"FeO"} + 2\ O_2 \overset{K_{G"}}{=} Fe_3O_4 \qquad (G")$$

where $K_{G"}$ represents the equilibrium constant of Eq.(G"). Since K_G equals to $K_{G"}$, the following equation may be written;

$$\log a_{Fe_3O_4} = 4.84 + 3 \log a_{\text{"FeO"}} + 1/2 \log Po_2 \qquad (H)$$

Let us use a schematic figure, Fig.I, of Fig.6 to explain the data easily. In addition, assuming that the activities of wustite $a_{\text{"FeO"}}$ on the isobaric lines of both AB and CD lines in Fig.I are equal (because vanadium content is little in wustite phase [maximum about 10%; see Table 6] and values of $\log a_{\text{"FeO"}}$ decreas with increase of vanadium content), the activities of magnetite in spinel solid solution series can be calculated by following equation similar to that described in Eq.(H);

$$\log a_{(Fe_3O_4)_{ss}} = 4.84 + 3 \log a_{\text{"FeO"}} + 1/2 \log Po_2 \qquad (H')$$

where $\log Po_2$ indicates the oxygen partial pressure at which both spinel and wustite solid solution phases coexist with in equilibrium. Also, mole fraction of (Fe_3O_4), $N_{Fe_3O_4}$, can be estimated at that oxygen pressure by using Fig. 8. Table 6 shows the activities of wustite on the AB line in Fig.I and the

Fig. I Schematic figure of Fig. 6.

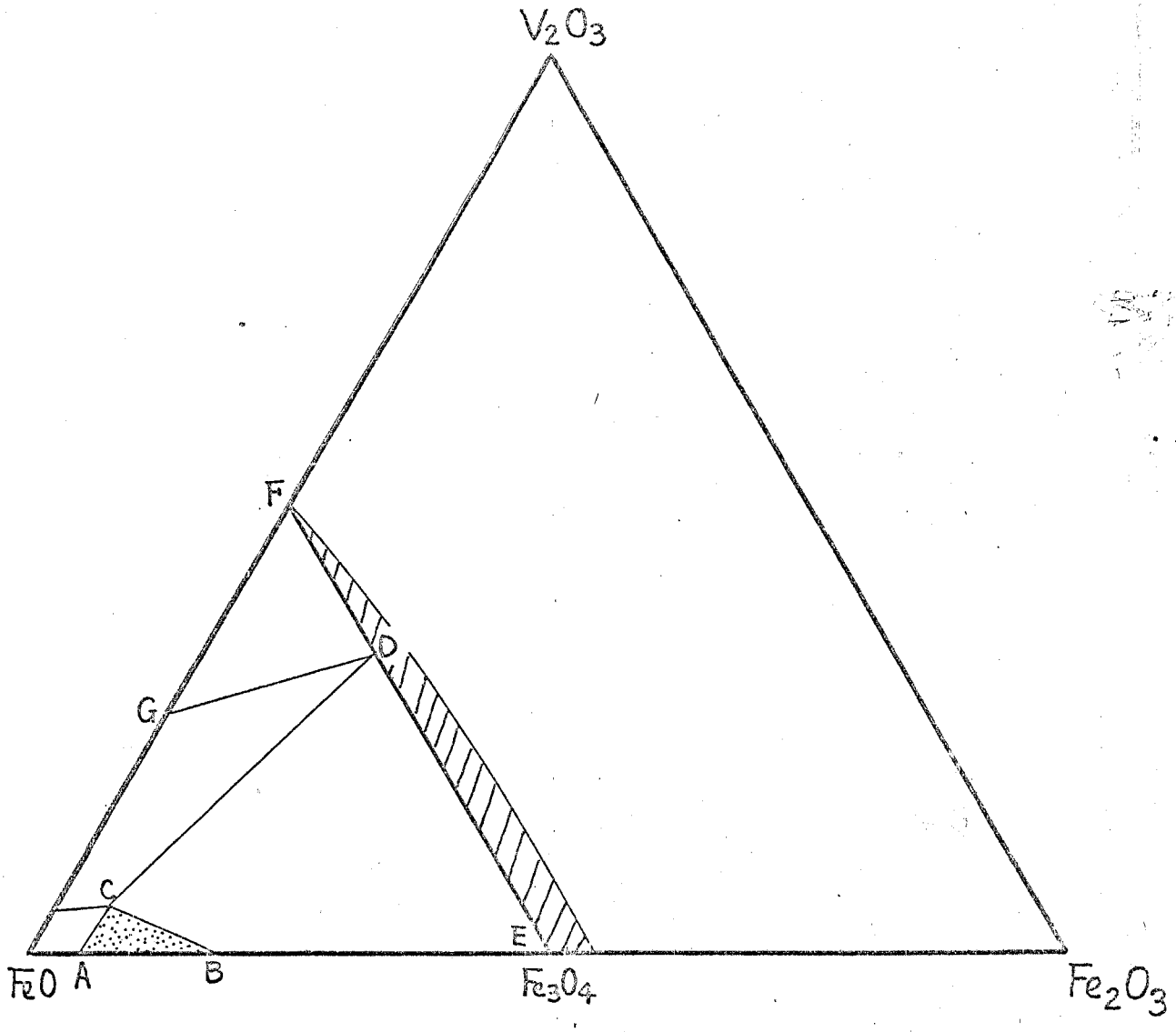

Table 6 Activities of wustite phase and related values at 1500°K

FeO mole %	Fe_2O_3 mole %	composition of FeO	- log Po_2	- log $a_{"FeO"}$	composition of (FeV)O and V/(Fe + V) **		mole fraction of magnetite in spinel
		$Fe_{0.855}O$	8.73	0.158 (0.156)*	$(Fe)_{0.855}O$	0	1
82.6	17.4	$Fe_{0.871}O$	9.01	0.118	$(FeV)_{0.912}O$	0.014	0.85
89.3	10.7	$Fe_{0.912}O$	10.04	0.043	$(FeV)_{0.883}O$	0.057	0.67
93.5	6.5	$Fe_{0.942}O$	10.94	0.008	$(FeV)_{0.900}O$	0.085	0.48
		$Fe_{0.954}O$	11.58	0	$(FeV)_{0.908}O$	0.099	0.33

** assume that activities on CD line equal to activities of AB line on the isobaric lines in Fig.I and Fig.6.

* data of Darken and Gurry

related values. As shown in Fig.6, the spinel solid solution phase coexists with wustite phase ranging from 1 to 0.33 mole fraction of magnetite (ED line in Fig.I). Calculated activities of magnetite $a_{(Fe_3O_4)_{ss}}$ in spinel solid solution are given in Table 7 together with related values.

Activities of magnetite on DF line are stable in equilibrium with metallic iron. Since vanadium compounds do not exist in the area DFG in Fig.I, the activities may be calculated by using Eq.(F): The equilibrium constant, K_F, can be obtained ;

$$\Delta G^{\circ}(F) = -152430 \pm 830 \text{ cal} = -RT \ln K_F$$

$$\log K_F = 22.21$$

Thus, following equation may be derived;

$$\log a_{Fe_3O_4} = \log K_F + 2 \log Po_2$$

$$= 22.21 + 2 \log Po_2 \qquad (I)$$

Therefore, activities of magnetite in the range 0-0.33 $N_{Fe_3O_4}$ can be calculated based on Eq.(I) and the oxygen partial pressures at which stoichiometric spinel and metallic iron coexist with in equilibrium. The activity data are summarized in Table 7 together with related values. Fig.9 shows the relation-

Table 7 Activities of magnetite in spinel solid solution series and the related constants at 1500°K

Fe_3O_4	- log "FeO"	- log Po_2	- log $a_{(Fe_3O_4)_{ss}}$	$a_{(Fe_3O_4)_s}$
1	0.158	8.73	0.001 = 0	1
0.85	0.118	9.01	0.019	9.57×10^{-1}
0.67	0.043	10.04	0.309	4.91×10^{-1}
0.48	0.008	10.94	0.654	2.22×10^{-1}
0.33	0	11.58	0.95	1.12×10^{-1}
0.20	-	12.25	2.29	5.13×10^{-3}
0.10	-	12.75	3.29	5.13×10^{-4}
0	-	13.25	4.29	5.13×10^{-5}

Fig. 9 Relationship between activity and mole fraction of magnetite in spinel solid solution series at 1500°K.

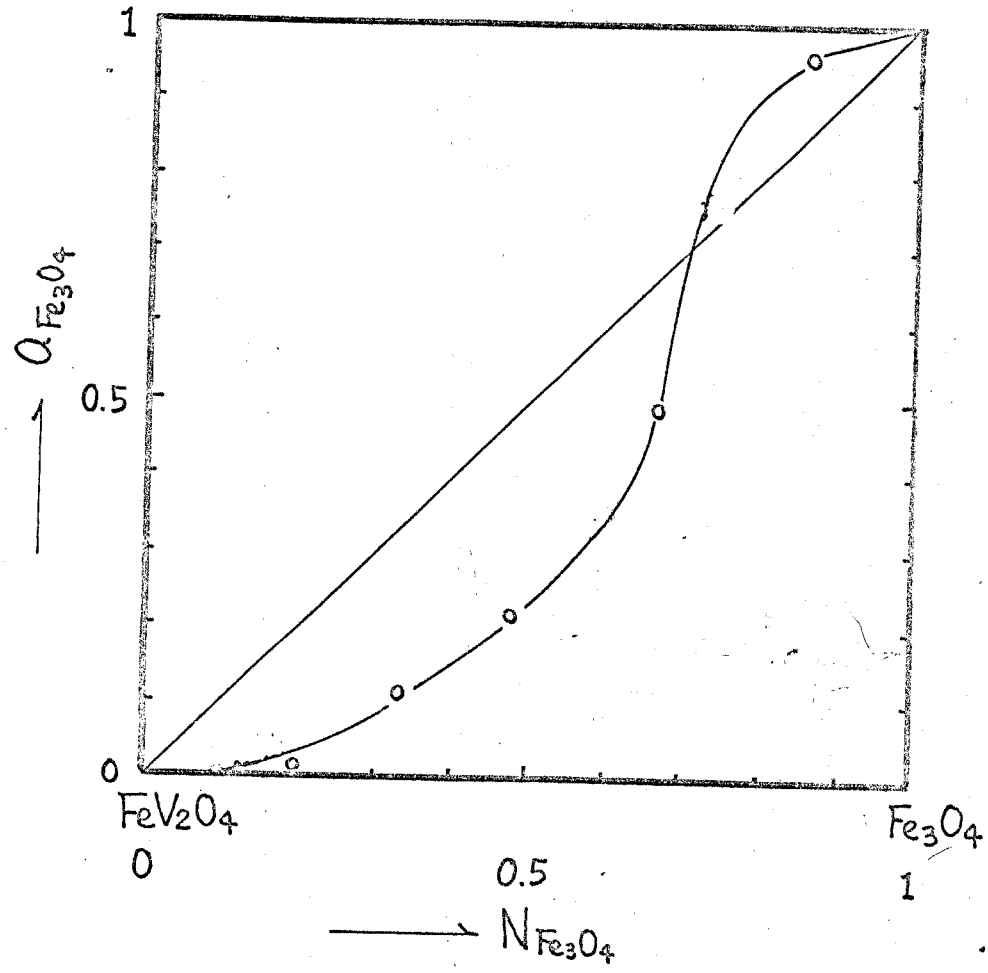

ship between activities of magnetite $a_{Fe_3O_4}$ and mole fraction of magnetite $N_{Fe_3O_4}$ in spinel solid solution series at 1500°K. The figure is similar to that of lattice parameter as will be shown in Fig.10. At any rate, the curve deviates from Raoult's law.

2-4) Summary ——— Equilibrium relations in the system FeO-Fe_2O_3-V_2O_3 have been determined at 1500°K by varying the oxygen partial pressure using gas mixtures of CO_2 and H_2 or CO_2 and O_2. The following oxide phases are stable under these conditions; a sesquioxide solid solution with corundom type structure (approximate composition Fe_2O_3-V_2O_3), a ternary solid solution with spinel structure (approximate composition $FeO\cdot Fe_2O_3$-$FeO\cdot V_2O_3$) and a ternary wustite solid solution with periclase type (MgO) structure and compositions approaching FeO. The extent of solid solution areas and the location of oxygen isobars have been determined. The standard free energy of FeV_2O_4 has been calculated based on the equilibrium oxygen partial pressure at which metallic iron and sesquioxide (V_2O_3) phases were stable in equilibrium. The activities of magnetite in spinel solid solution series have been calculated at 1500°K based on the several oxidation reactions. Activities versus composition relations have deviated from Raoult's law.

CHAPTER 3

Magnetic Properties of the FeV_2O_4-Fe_3O_4 System

3-1 INTRODUCTION

The phase equilibria on the solid solution system of FeV_2O_4-Fe_3O_4 have been described in Chapter 2.

Since the FeV_2O_4 and Fe_3O_4 have a normal [43] and an inverse[44] spinel structure, respectively, the FeV_2O_4-Fe_3O_4 system may be expected interesting magnetic properties. The magnetic properties of FeV_2O_4 and Fe_2VO_4 were studied by Wold et al[45]. They reported that a Curie point for FeV_2O_4 of 109°K and a saturation moment at 4.2°K of 1.95 μ_B (Bohr magnetons) per formula unit; those for Fe_2VO_4 are 440°K and 0.72 μ_B, respectively. Recently, the ionic configuration in Fe_2VO_4 was proposed to be $Fe^{3+}(Fe^{2+}V^{3+})O_4$ by Bernier and Poix[46] based on their anion-cation distance calculation method and studies of various magnetic properties. Magnetic and elecric properties of the spinel solid solution $Fe_{1+\lambda}V_{2-\lambda}O_4$ ($0 \leqq \lambda \leqq 1$) were studied by Rogers et al[47]. They reported that there was an abnormal electric behaviour in the vicinity of FeV_2O_4. The Mössbauer spectra of this solid solution series were measured by Rossiter[48] and cation distributions of $Fe^{2+}(Fe^{3+}_{\lambda}V^{3+}_{2-\lambda})O_4$ ($0 \leqq \lambda \leqq 1$) were proposed for this system. Samples used above studies seem to be uncertain whether or not they are of accu-

rately stoichiometric composition and of pure phase.

The purpose of the present study is to prepare the stoichiometric spinel solid solution series of FeV_2O_4-Fe_3O_4 system under controlled CO_2-H_2 atmospheres at 1500°K and to investigate the lattice parameters and magnetic properties of the system for the temperature range from 77°K (liquid nitrogen temperature) to 860°K.

3-2 EXPERIMENTAL

3-a) Sample Preparation ——— Samples of the FeV_2O_4-Fe_3O_4 spinel solid solution series used in the present study were prepared at 1500°K according to the procedures which were described in Chapter 2 (2-b). The equilibrated sample was quenched in a suitable oxygen pressure under which the sample had a stoichiometric composition. The oxygen partial pressure was controlled based on the results of thermogravimetry as shown in Fig.8. Total compositions of the quenched sample were determined by means of the gravimetric weight gain method as described in Chapter 2 (2-c) to ensure whether the sample was a stoichiometric composition or not.

3-b) Identification of Phases ——— The spinel phase present in the quenched sample was identified by an X-ray diffraction method using Fe K_α radiation. Silicon powder was used as the standard in determining d values of the phase present.

3-c) Magnetic Measurements ———. The magnetization of samples was determined by the Faraday method. The force, the e.m.f. of the thermocouple attached on the specimen, and the current intensity of the applied field were automatically recorded by a suitable recording device. The maximum value of the field was approximately 7000 Oe. Calibration of the magnetization was carried out by using nikel powder

with a purity of 99.99 %, which has the value of 0.5714 μ_B per atom[49] at 293°K. The error of the measured magnetization for each specimen was estimated to be within ± 3 per cent. The experimental formula, $M_h = M_s(1 - \text{const}\cdot H^{-1})$ was used to correct the observed magnetization at 77°K to the saturation magnetization at 77°K. Where both M_h and M_s indicate a moment at any valu of H (magnetic field) at 77°K and the saturation moment at 77°K, respectively. A value of M_s for each specimen was graphically taken as the intercept on the M_h axis by extrapolating a value of H^{-1} to zero (or by choosing a value of H as infinity). No extrapolation to the saturation moment at 0°K was carried out because magnetization curves of FeV_2O_4, or those close to the composition, and $Fe_{1.8}V_{1.2}O_4$ were difficult to assume their behaviour in the temperature range from 77° to 0°K, as will be shown in Fig.11(b) and Fig.11(c).

Pt-13%Rh and Au·2%Co-Cu thermocouples were used to measure temperature above and below room temperature, respectively. The variation of temperatures between 77° and 860°K was achieved by use of suitable Dewar vessel and non-inductive electric furnace. Temperature calibration was carried out at the liquid N_2 temperature and at the freezing point of water for the Au·2%Co-Cu thermocouple; at the Curie temperatures of pure nickel (546°K) and stoichiometric magnetite (851°K) for the Pt-13%Rh·Pt thermocouple. The temperature is correct within an accuracy of ± 5°K.

3-3 RESULTS AND DISCUSSION

1) Samples ——— Specimens were prepared in the most suitable oxygen partial pressure under which the spinel existed in the stoichiometric composition in equilibrium state at 1500°K. The values of oxygen partial pressure at which sample was prepared are listed in Table 8.

2) Lattice Parameter ——— Lattice parameters for the prepared samples are given in Table 8 and Fig.10. The relation between lattice parameter and composition parameter x ($0 \leqq x \leqq 1$) deviates considerably from Vegard's law. In the range $0 \leqq x \leqq 0.5$, they are in good agreement with those of Rogers et al.[47] and Rossiter[48]. In the range $0.5 \leqq x \leqq 1$, however, the parameter decreases with a gentler slope than in the range $0 \leqq x \leqq 0.5$, and the results are sightly different from the work by Vorob'ev et al[37].

3) Magnetic Properties ——— The magnetizations of a number of spinels were measured between 77°K and their Curie temperatures. Typical examples of magnetization versus temperature are shown in Fig.11(a)-(c). In Fig.11(a), the magnetizations decrease smoothly with increase of temperature. Similar temperature dependence of magnetizations was observed for the compositional range $0.44 \leqq x \leqq 1$. In the Fe_2VO_4 (x=0.5), the curve agrees well with that examined by Bernier and Poix[46] in

Table 8 Values of constants for some members of the FeV_2O_4-Fe_3O_4 system

$Fe_{1+2x}V_{2-2x}O_4$		atmospheric condition	lattice parameter	saturation magnetization in μ_B	Curie temp.
value of x	compound	$-\log Po_2 \pm 0.05$	a_o (Å)	per formula unit 77^oK	$(^oK) \pm 5^o$
0	FeV_2O_4	13.08	8.452 ± 0.001	1.54	127
0.0625	$Fe_{1.125}V_{1.875}O_4$	12.03	8.450 ± 0.002	1.49	121
0.1	$Fe_{1.2}V_{1.8}O_4$	11.90	8.450 ± 0.002	1.39	132
0.175	$Fe_{1.35}V_{1.65}O_4$	11.90	8.450 ± 0.002	1.08	170
0.25	$Fe_{1.5}V_{1.5}O_4$	10.90	8.446 ± 0.002	0.72	222
0.325	$Fe_{1.65}V_{1.35}O_4$	10.90	8.441 ± 0.002	0.294	295
0.3625	$Fe_{1.725}V_{1.275}O_4$	10.90	-	0.142	333
0.4	$Fe_{1.8}V_{1.2}O_4$	10.45	8.426 ± 0.002	0.044	358
0.4375	$Fe_{1.875}V_{1.125}O_4$	10.45	-	0.253	-
0.475	$Fe_{1.95}V_{1.05}O_4$	10.15	-	0.50	432
0.5	Fe_2VO_4	9.72	8.418 ± 0.002	0.73	454
0.55	$Fe_{2.1}V_{0.9}O_4$	9.72	-	0.98	516
0.625	$Fe_{2.25}V_{0.75}O_4$	9.72	8.408 ± 0.002	1.40	566
0.7	$Fe_{2.4}V_{0.6}O_4$	9.17	8.407 ± 0.002	2.02	621
0.775	$Fe_{2.55}V_{0.45}O_4$	8.89	8.401 ± 0.001	2.34	698
0.8125	$Fe_{2.625}V_{0.375}O_4$	8.89	-	2.85	-
0.85	$Fe_{2.7}V_{0.3}O_4$	8.89	8.399 ± 0.002	3.05	738
0.8375	$Fe_{2.775}V_{0.225}O_4$	8.89	8.396 ± 0.001	3.19	-
0.925	$Fe_{2.85}V_{0.15}O_4$	8.50	8.395 ± 0.002	3.42	814
1.0	Fe_3O_4	8.10	8.394 ± 0.002	4.03	851

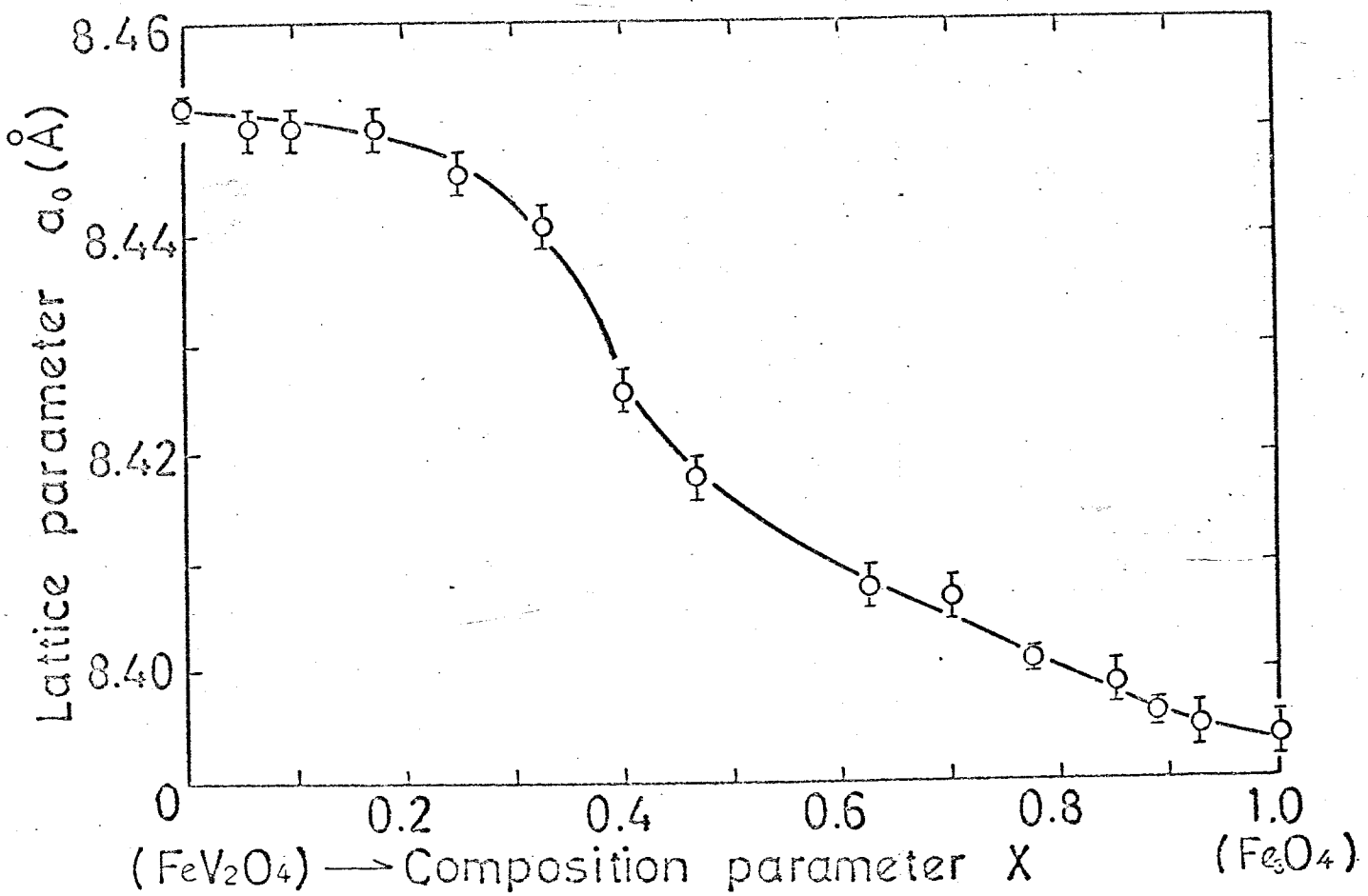

Fig. 10 Relationship between lattice parameter and composition parameter x for the system $Fe_{1+2x}V_{2-2x}O_4$ ($0 \leqq x \leqq 1$).

Fig.11(a)

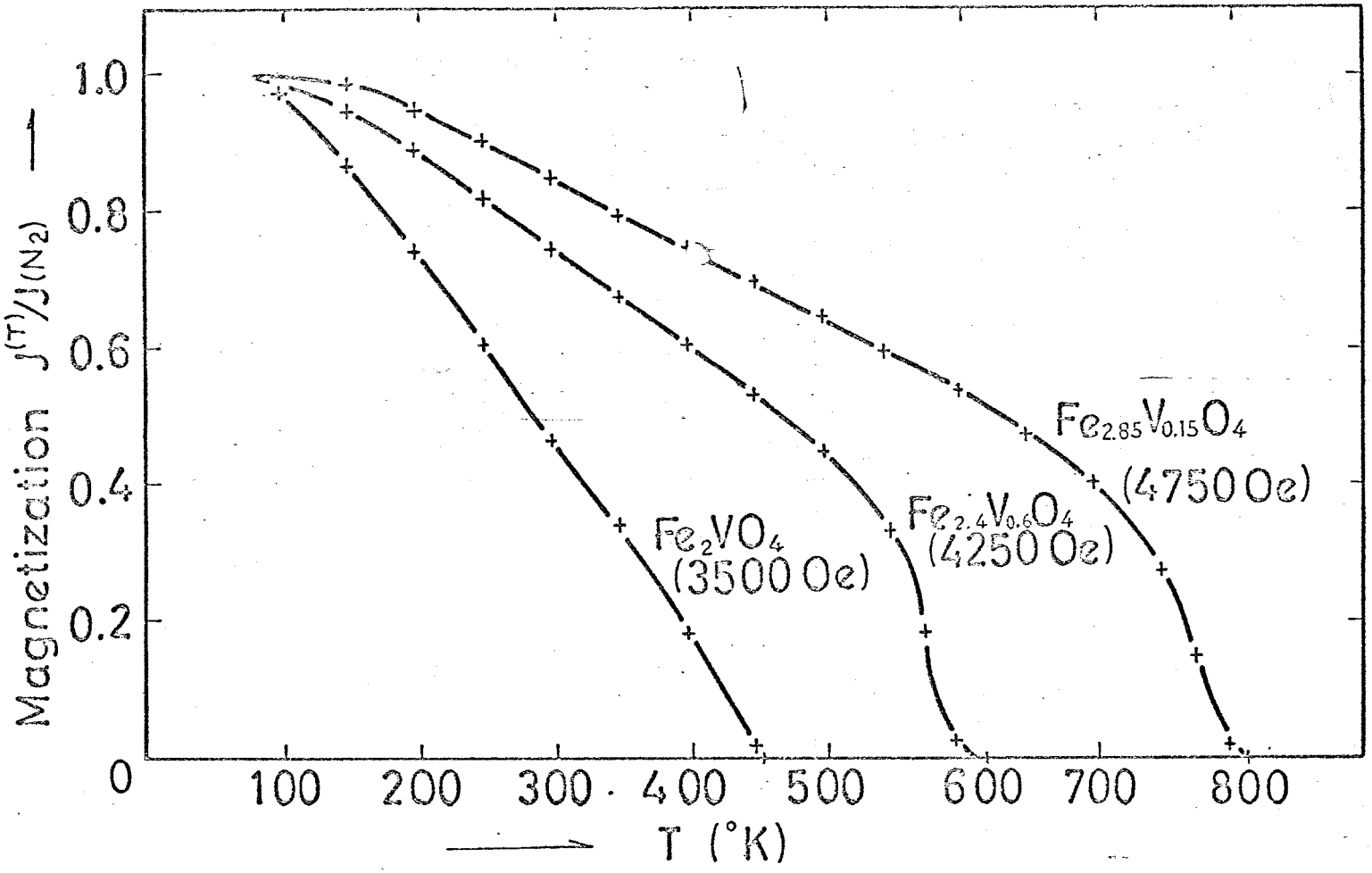

Fig.11(a)-(c) Magnetization curves with temperature for several compositions of spinels taken the magnetization at 77°K as a reference.

Fig.11(b)

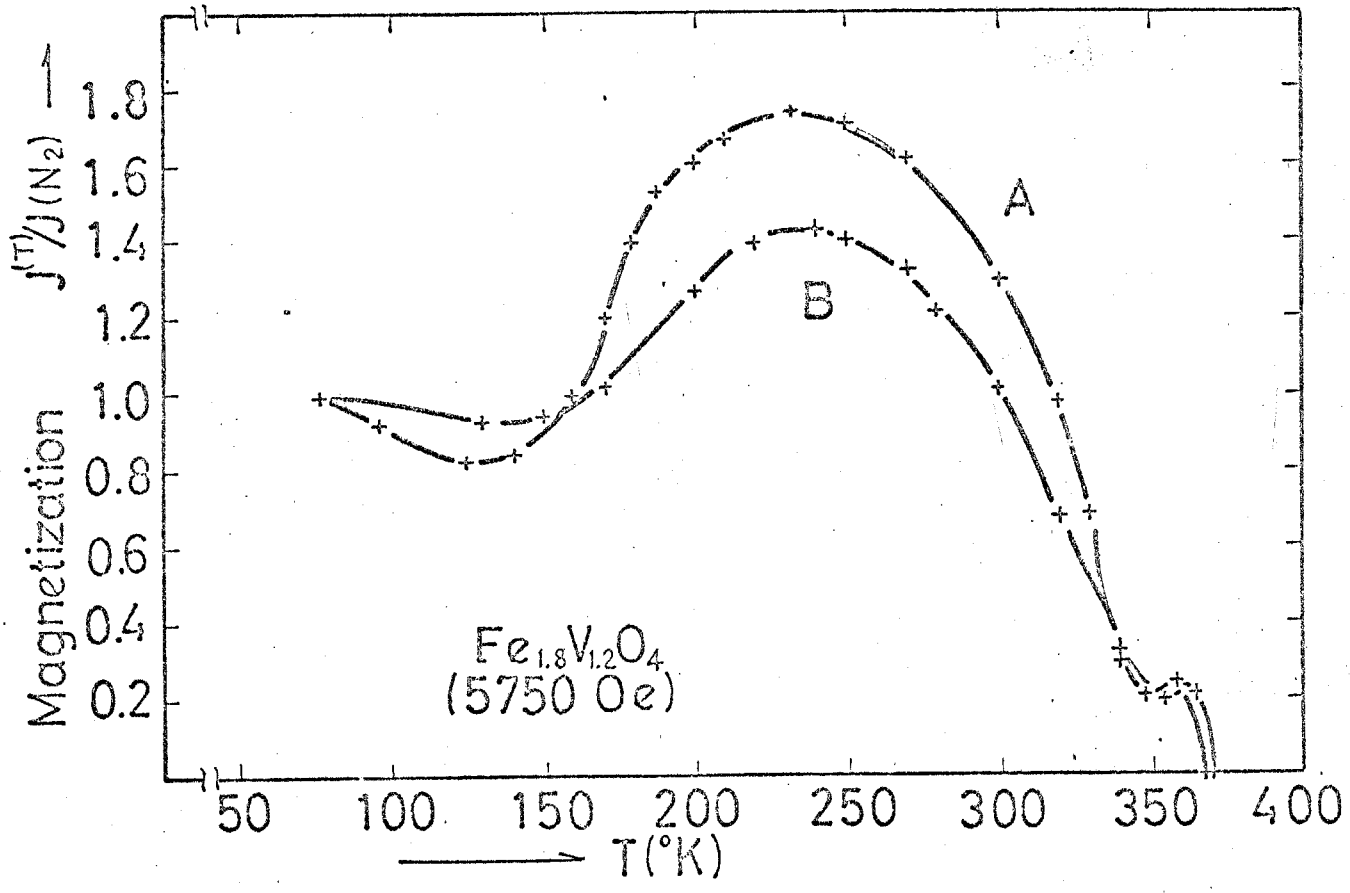
Magnetization J(T)/J(N2)
1.8
1.6
1.4
1.2
1.0
0.8
0.6
0.4
0.2
A
B
Fe1.8V1.2O4
(5750 Oe)
50
100
150
200
250
300
350
400
T(°K)

Fig.11(c)

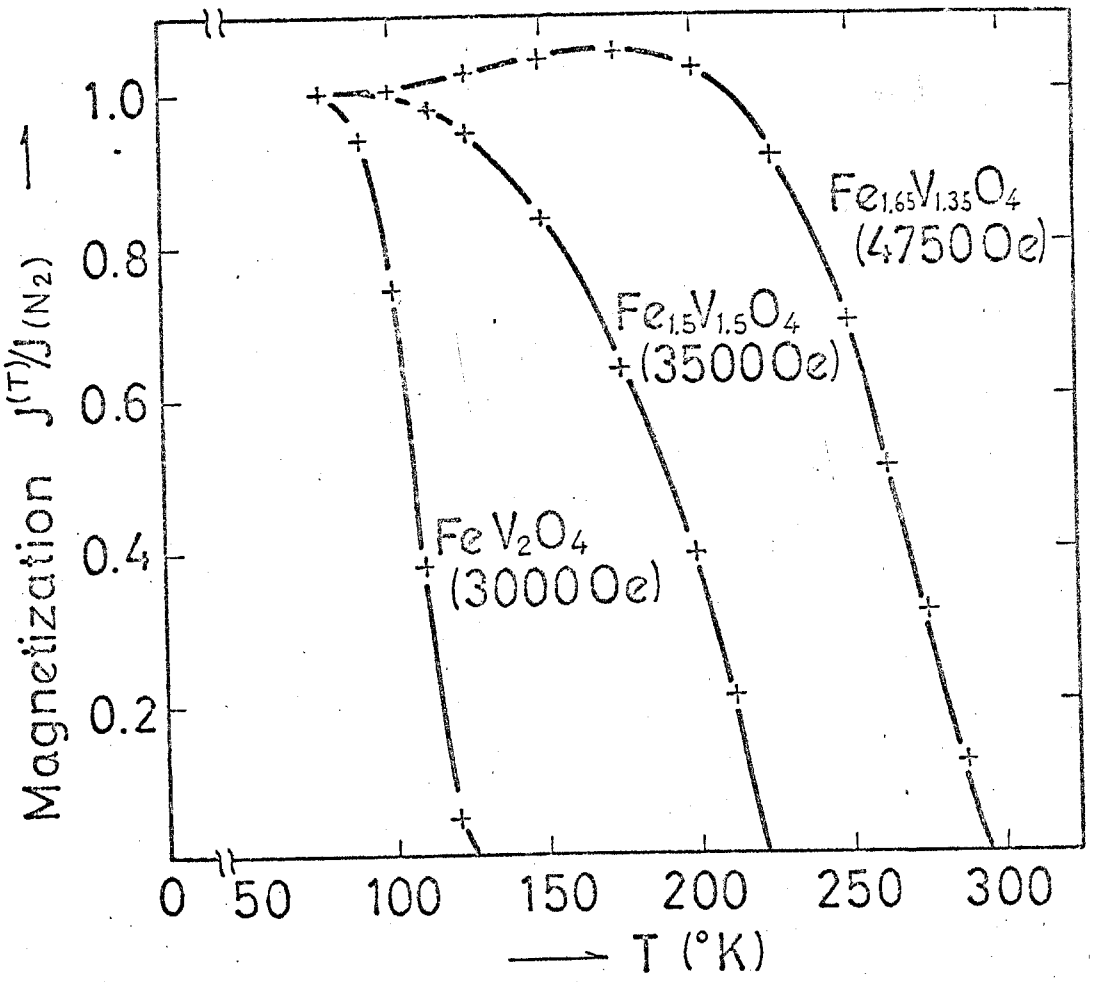
Magnetization $J^{(T)}/J_{(N_2)}$
1.0
0.8
0.6
0.4
0.2
0
50
100
150
200
250
300
T (°K)
$Fe_{1.65}V_{1.35}O_4$ (4750 Oe)
$Fe_{1.5}V_{1.5}O_4$ (3500 Oe)
FeV_2O_4 (3000 Oe)

the field of 26000 Oe and down to 40°K. The magnetization for the specimen $Fe_{1.8}V_{1.2}O_4$ (x = 0.4) is shown in Fig.11(b); here sample A was left in a furnace for a longer time than that of B at 1500°K after the equilibrium was attained. The curves show the complex behaviours. This composition, $Fe_{1.8}V_{1.2}O_4$, also corresponds to the minimum value of the magnetic moment (0.044 μ_B) at 77°K as will be illustrated in Fig.13 and tabulated in Table 8. Similar J(T) curves were observed in the specimens within $0.33 \leqq x \leqq 0.4$. One of the curve ($Fe_{1.65}V_{1.35}O_4$, x = 0.325), is shown in Fig.11(c). In the specimens within $0 \leqq x \leqq 0.25$, the variations of magnetization are similar to those of examples, $Fe_{1.5}V_{1.5}O_4$ (x = 0.25) and FeV_2O_4 (x = 0), shown in Fig.11(c). In those specimens, the Curie temperatures are too low to evaluate the value of the saturation magnetization at 0°K from the data obtained above 77°K. Therefore, in these compositional ranges, the measurement of magnetization between liquid helium temperature and the Curie temperature seems to be necessary to ensure the saturation magnetization.

The Curie points for the present solid solution are illustrated in Fig.12 and in Table 8. As seen in Fig.12, the Curie points increase almost linearly with x for the system $Fe_{1+2x}V_{2-2x}O_4$ in the range from 0.1 to 1, while they are almost constant in the vicinity of FeV_2O_4. The Curie points of FeV_2O_4 and Fe_2VO_4 are 127° and 454°K, respectively. These values are slightly higher than the data obtained by Wold et al[45].

Fig.13 illustrates the relationship between the corrected

Fig.12 The Curie temperature vs composition parameter x for the system $Fe_{1+2x}V_{2-2x}O_4$ ($0 \leq x \leq 1$).

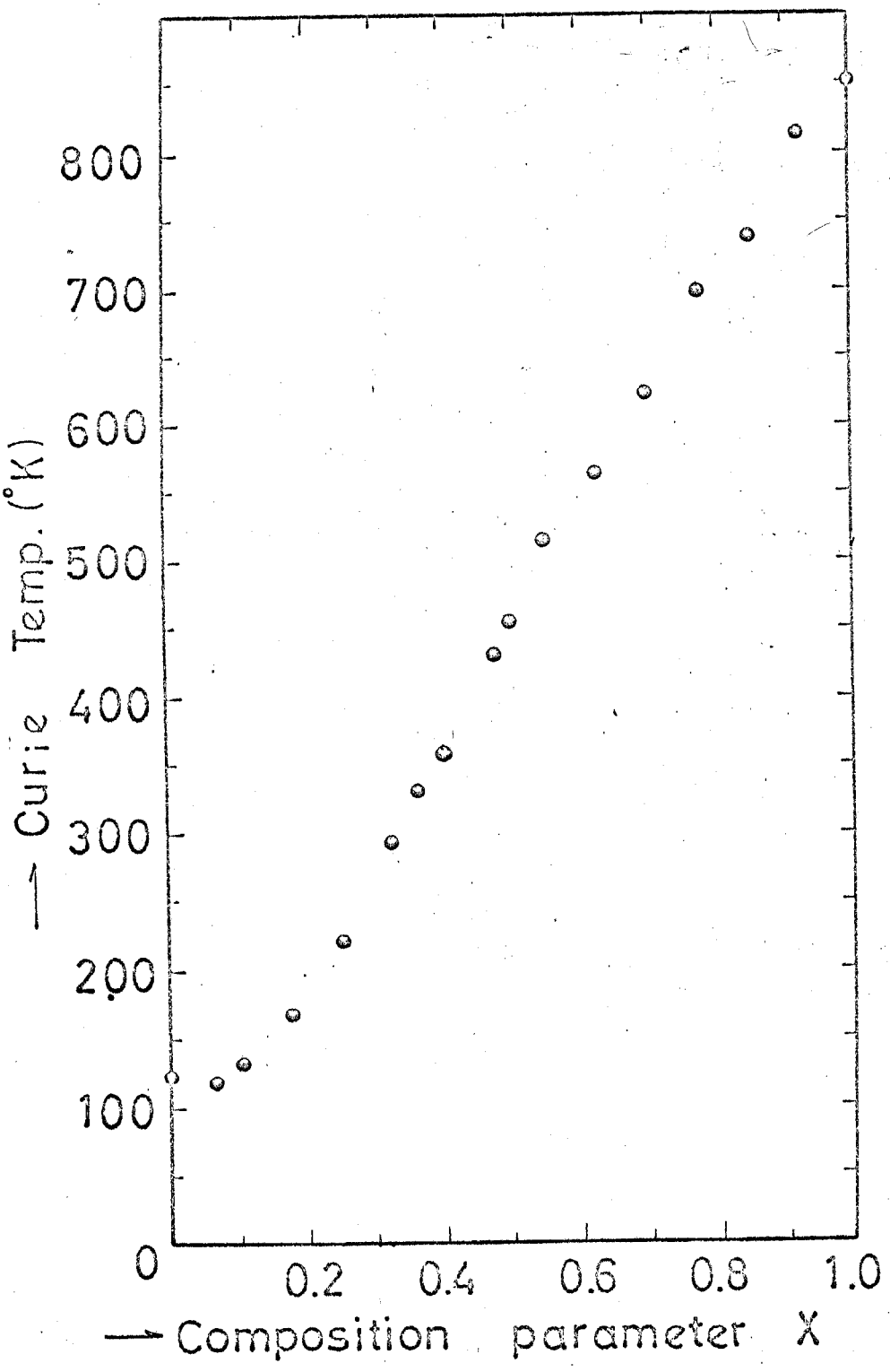

saturation moment in μ_B per formula unit at 77°K and x ($0 \leqq x \leqq 1$) for the system $Fe_{1+2x}V_{2-2x}O_4$. The values of saturation moment are also tabulated in Table 8. The magnetic moment decreases almost linearly with decrease of x and becomes almost zero at the composition, $Fe_{1.8}V_{1.2}O_4$; it then increases again toward FeV_2O_4.

In order to consider the cation distributions and the magnetic structure of the system $Fe_{1+2x}V_{2-2x}O_4$ without difficulty, let us divide it into two parts, the subsystems Fe_2VO_4-Fe_3O_4 and FeV_2O_4-Fe_2VO_4.

Magnetite, Fe_3O_4, is well known to be an inverse spinel with ferrous iron in octahedral sites[44]. Five models of cation distributions for Fe_2VO_4-Fe_3O_4 solid solution series may be possible as illustrated in Table 9, where outside and inside ions of the parenthesis denote ions occupying A (tetrahedral) and B (octahedral) sites, respectively. μ is the composition parameter and varies from 0 to 1. The values of magnetic moment, Fe^{2+}, Fe^{3+} and V^{4+} ions are, assuming spin only values, 4.0, 5.0 and 1.0 μ_B per ion, respectively. Goodenough[50] has given 1.40 μ_B per ion for the magnetic moment of V^{3+} ions at B site. An equation to calculate magnetic moments for the solid solution Fe_2VO_4-Fe_3O_4 is easily derived from the difference of the moments between A and B sites by assuming antiparallel coupling of sublattice moments between A and B sites and by using moments for each ion as described above. Equations of the magnetic moments for each of five models are also illus-

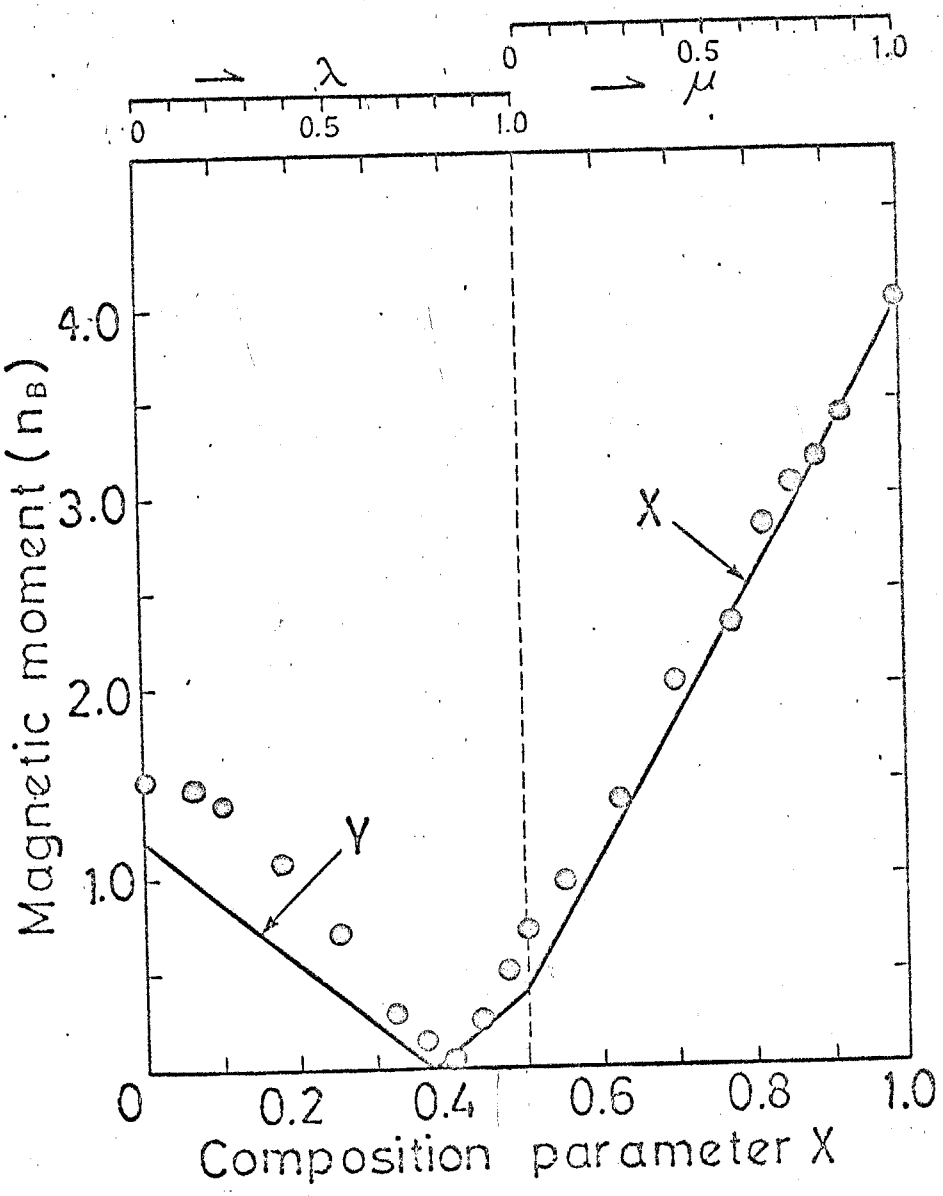

Fig.13 Relationship between corrected saturation moments in μ_B (Bohr magnetons) per molecule at 77°K and composition parameter μ ($0 \leqq \mu \leqq 1$) and λ ($0 \leqq \lambda \leqq 1$) according to the models of $Fe^{3+}(Fe^{2+}_{\mu}Fe^{3+}_{1-\mu}V^{3+})O_4$ and $Fe^{3+}_{\lambda}Fe^{2+}_{1-\lambda}(Fe^{2+}_{\lambda}V^{3+}_{2-\lambda})O_4$, respectively.

Table 9 Possible cation distributions for the Fe_2VO_4-Fe_3O_4 and equations to calculate magnetic moments per formula unit when Fe^{3+}, Fe^{2+}, V^{4+} and V^{3+} are given by 5.0, 4.0, 1.0 and 1.4 μ_B, respectively; μ changes in the range $0 \leqq \mu \leqq 1$ and S_a and S_b represent the moments both A site and B site, respectively.

model	
1	$V^{4+}_{1-\mu}Fe^{3+}(Fe^{2+}Fe^{2+}_{1-\mu}Fe^{3+}_{\mu})O_4$
	$X = S_b - S_a = -3.0\cdot\mu + 7.0$
2	$Fe^{2+}_{1-\mu}Fe^{3+}_{\mu}(Fe^{2+}Fe^{3+}_{\mu}V^{4+}_{1-\mu})O_4$
	$X = S_b - S_a = 3.0\cdot\mu + 1.0$
3	$Fe^{3+}(Fe^{2+}Fe^{3+}_{\mu}V^{3+}_{1-\mu})O_4$
	$X = S_b - S_a = 3.6\cdot\mu + 0.4$
4	$Fe^{3+}_{\mu}V^{3+}_{1-\mu}(Fe^{2+}Fe^{3+})O_4$
	$X = S_b - S_a = -3.6\cdot\mu + 7.6$
5	$Fe^{2+}_{1-\mu}Fe^{3+}_{\mu}(Fe^{3+}Fe^{2+}_{\mu}V^{3+}_{1-\mu})O_4$
	$X = S_b - S_a = 1.6\cdot\mu + 2.4$

trated in Table 9, where S_a and S_b represent magnetic moments of A and B sites, respectively. The calculated moments using models of 1, 4 and 5 markedly deviate from the measured moments. On the other hand, the calculated moments using equations for models of 2 and 3 are in reasonable agreement with observed ones.

FeV_2O_4 is known from the X-ray diffraction results to be normal with ferrous iron in tetrahedral sites[43]. Hence, two cation distributions for FeV_2O_4-Fe_2VO_4 solid solution are possible as the results of the above suitable models, 2 and 3.

a) $Fe^{2+}(V^{3+}V^{3+})O_4 \longrightarrow Fe^{2+}(Fe^{2+}V^{4+})O_4$

b) $Fe^{2+}(V^{3+}V^{3+})O_4 \longrightarrow Fe^{3+}(Fe^{2+}V^{3+})O_4$

The general formula for the cation distributions of (a) can be written as $Fe^{2+}(Fe^{2+}_{\lambda}V^{3+}_{2-2\lambda}V^{4+}_{\lambda})O_4$ $(0 \leqq \lambda \leqq 1)$. The calculated magnetic moment on this model is evaluated from the following equation;

$$Y = |S_b - S_a| = |2.2\lambda - 1.2| \qquad (0 \leqq \lambda \leqq 1) \qquad (24)$$

where S_a and S_b represent magnetic moments on A site and B site, respectively. λ is the composition parameter varying from 0 to 1. Similarly, the model for cation distributions of (b) can be written as $Fe^{3+}_{\lambda}Fe^{2+}_{1-\lambda}(Fe^{2+}_{\lambda}V^{3+}_{2-\lambda})O_4$ $(0 \leqq \lambda \leqq 1)$. The equation to calculate moments on this model is given by

follows;

$$Y = \left| S_b - S_a \right| = \left| 1.6\lambda - 1.2 \right| \qquad (0 \leqq \lambda \leqq 1) \qquad (25)$$

Eq.(25) agrees better with the observed moments than Eq.(24) as shown in Fig.13 where the data points are taken from Table 8. In the vicinity of Fe_2VO_4, lattice parameters, the Curie points and magnetic moments vary continuously with x as shown in Figs. 10, 12 and 13. Therefore, remarkably different cation distributions can not be considered on either side of Fe_2VO_4. Also, the lattice parameters indicate rapid change in the compositional range, $x \leqq 0.5$, compared with that in the compositional range, $0.5 \leqq x \leqq 1$, as shown in Fig.10. This may be consistent with the assumption of model (b) that Fe^{2+} ions (ionic radius; 0.83 Å) replace Fe^{3+} ions (ionic radius; 0.67 Å) in A sites. Thus, it may be concluded that the cation distributions of $Fe^{3+}(Fe^{2+}Fe^{3+}_{\mu}V^{3+}_{1-\mu})O_4$ and $Fe^{3+}_{\lambda}Fe^{2+}_{1-\lambda}(Fe^{2+}_{\lambda}V^{3+}_{2-\lambda})O_4$ are suitable for Fe_2VO_4-Fe_3O_4 and FeV_2O_4-Fe_2VO_4 subsystems, respectively. As a result, it should be noted that both Fe^{2+} and V^{3+} ions prefer B sites to A sites through all the system of $Fe_{1+2x}V_{2-2x}O_4$ $(0 \leqq x \leqq 1)$. The equation of model 2 in Table 9 and Eq.(25) are indicated by a solid line X and a folded line Y, respectively, in Fig.13. The measured saturation moments for the FeV_2O_4-Fe_2VO_4 solid solution indicate a significant deviation from the folded line Y in the compositional range, FeV_2O_4-$Fe_{1.5}V_{1.5}O_4$. The disagreement between the observed and the calculated saturation

moments may be partly due to a noncollinear spin configuration in the FeV_2O_4-Fe_2VO_4 spinel solid solution series and partly due to uncertainty of the corrected saturation moments in the vicinity of FeV_2O_4. Indeed, Menyuk et al.[51] and Dwight et al.[52] studied the magnetic properties of the normal cubic spinels MnV_2O_4 and CoV_2O_4, and recognized that these spinels have not a Néel type configuration at low temperature (4.2°K). They also mentioned that the effect is attributed to the importance of orbital degeneracy and spin-orbit coupling in connection with V^{3+} ions.

Rossiter[48] proposed the model of $Fe^{2+}(Fe^{3+}_{\lambda}V^{3+}_{2-\lambda})O_4$ ($0 \leqq \lambda \leqq 1$) for the FeV_2O_4-Fe_2VO_4 solid solution series based on his Mössbauer spectra study. However, the corresponding equation, $Y = |S_b - S_a| = |3.6\lambda - 1.2|$ ($0 \leqq \lambda \leqq 1$), which assumes ferrimagnetic coupling, deviates extreamely from this study. Bernier and Poix[47] proposed $Fe^{3+}(Fe^{2+}V^{3+})O_4$ for Fe_2VO_4 based on the structual and magnetic properties of this compound. Their conclusion is consisted with this study in the composition Fe_2VO_4.

Thus, it seems that in the FeV_2O_4-Fe_3O_4 solid solution system, Néel's ferrimagnetic AB coupling is sufficiently large to keep linear spin configuration if Fe^{2+} ions occupy half of the B sites, but AB coupling becomes weak and in turn BB coupling becomes compatible with it if V^{3+} ions occupy more than half of the B sites.

3-4) Summary ——— A series of spinel having stoichiometric composition in the FeV_2O_4-Fe_3O_4 system has been prepared at 1500°K under controlled CO_2-H_2 atmospheres. The relationship between lattice parameter and composition of the spinel solid solution system showed a significant deviation from Vegard's law, and the Curie temperatures varied with composition almost linearly except for the composition in the vicinity of FeV_2O_4. A minimum value of saturation moment, approximate 0.04 μ_B per formula unit, was observed at the composition $Fe_{1.8}V_{1.2}O_4$. Saturation magnetization was reasonably explained by assuming the cation distributions as $Fe^{3+}(Fe^{2+}_{\mu}Fe^{3+}_{1-\mu}V^{3+}_{1-\mu})O_4$ $(0 \leqq \mu \leqq 1)$ for the Fe_2VO_4-Fe_3O_4 solid solution, and $Fe^{3+}_{\lambda}Fe^{2+}_{1-\lambda}(Fe^{2+}_{\lambda}V^{3+}_{2-\lambda})O_4$ $(0 \leqq \lambda \leqq 1)$ for the FeV_2O_4-Fe_2VO_4.

REFERENCES

1) W.Klemm and L.Grimm, Z. anorg. u. allgem. Chem., 250, 42 (1942)
2) A.U.Seybolt and H.T.Sumision, J. Metals, 5, 292 (1953).
3) E.Hoschek and W.Klemm, Z. anorg. u. allgem. Chem., 242, 63 (1939).
4) F.Aebi, Helv. Chim. Acta, 31, 8 (1948).
5) G.Andersson, Acta Chem. Scand., 8, 1599 (1954).
6) G.Andersson, ibid., 10, 623 (1956).
7) S.Andersson, ibid., 14, 1161 (1960).
8) K.Kosuge, T.Takada and Y.Kachi, Nippon Kagaku Zasshi (J. Chem. Soc. Japan, Pure Chem. Sect.1, 83, 1243 (1962).
9) K.Kosuge, J. Phys. Chem. Solids, 28, 1613 (1967).
10) S.Kachi and R.Roy, Second Quarterly Report on Crystal Chemistry Studies, Pennsylvania State University, 4 December (1965).
11) J.P.Coughlin, Bureau of Mines, Bull., 542, U.S.A. (1954).
12) T.Katsura and M.Hasegawa, J. Chem. Soc. Japan, 40, 561 (1967).
13) A.Burdese, Ann. Chim.(Rome), 47, 785 (1957).
14) G.Grossmann, O.W.Proskurenko and Ss. M.Arija, Z. anorg. u. allgem. Chem., 305, 121 (1960).
15) J.S.Andersson and A.S.Khan, J. Less Common Metals, 22, 209 (1970).
16) T.Katsura and A.Muan, Trans. A.I.M.E., 230, 77 (1964).
17) T.Katsura and S.Kimura, J. Chem. Soc. Japan, 38, 1664 (1965).
18) L.S.Darken and R.W.Gurry, J. Am. Chem. Soc., 67, 1398 (1945); ibid., 68, 798 (1946).
19) J.F.Elliott and M.Gleiser, "Thermochemistry for Steel Making" Addison Wesley, New York (1960).
20) E.Bauer and H.Preis, Z. Electrochem., 43, 727 (1937).
21) C.Wagner, Naturwissenshaften, 23/24, 265 (1943).
22) F.Hund, Z. Phys. Chem., 199, 142 (1952).
23) J.Weissbart and R.Ruka, Rev. Sci. Instr., 32, 593 (1961).
24) J.Weissbart and R.Ruka, J. Electrochem. Soc., 109, 723 (1962).

25) K.Kiukkola and C.Wagner, J.Electrochem. Soc., 104, 379 (1957).
26) W.D.Kingery, J.Pappis, M.E.Dotty and D.C.Hill, J. Am. Ceram. Soc., 42, 393 (1959).
27) H.A.Jahanson and J.G.Cleary, J. Elecrochem. Soc., 111, 100 (1964).
28) G.G.Charette and S.N.Flengas, ibid., 115, 796 (1968).
29) T.Nakazono, J. Chem. Soc. Japan, 42, 761 (1921).
30) I.Iwasaki, T.Katsura, M.Yoshida and T.Tarutani, Japan Analyst, 6, 211 (1957).
31) R.C.Evans, "An Introduction to Crystal Chemistry" Cambridge University Press (1966).
32) H.Siemonsen and H.Ulich, Z. Electrochem., 46, 141 (1940).
33) K.K.Kelley and E.G.King, "Contributions to the Data on Theoretical Metallurgy. X. Heat-Content, Heat-Capacity, and Entropy data for Inorganic Substances", Bull., 476, Bureau of Mines, U.S.A. (1949).
34) J.Smiltens, J. Am. Chem. Soc., 79, 4877 (1957).
35) W.Nernst, "Theoretische Chemie" F.Enke, Stuttgart, (1926).
36) A.Rahmel, W.Jäger and R.Korn, Arch. Eisenhutten Wes. 34, 279 (1963).
37) Yu.P.Vorob'ev, V.N.Bogoslovskii, E.G.Bogachova and G.I.Chufarov Dokl. Akad. Nauk, S.S.S.R., 166, 664 (1966).
38) W.Kunnmann, D.B.Rogers and A.Wold, J. Phys. Chem. Solids, 24, 1535 (1963).
39) G.Schmahl and H.Dillenburg, Z. Phys. Chem., 65, 119 (1969).
40) D.E.Cox, W.J.Takei, R.C.Miller and G.Shirane, J. Phys. Chem. Solids, 23, 863 (1962).
41) R.W.Taylor, Am. Mineral., 49, 1016 (1964).
42) M.Wakihara and T.Katsura, Met. Trans., 1, 363 (1970).
43) H.M.Richardson, F.Ball and G.R.Rigby, Trans. Brit. Ceram. Soc. 50, 376 (1954).
44) E.J.W.Verwey and E.L.Heilmann, J. Chem. Phys., 15, 174 (1947).
45) A.Wold, D.Rogers, R.J.Arnott and N.Menyuk, J. Appl. Phys., 33, 1208 (1962).

46) J.C.Bernier and P.Poix, Ann. Chim., 2, 81 (1967).
47) D.B.Rogers, R.J.Arnott, A.Wold and J.B.Goodenough, J. Phys. Chem. Solids, 24, 347 (1963).
48) M.J.Rossiter, J. Phys. Chem. Solids, 26, 775 (1965).
49) E.C.Stoner, "Magnetism and Matter" pp383-4, Methuen, London (1934).
50) J.B.Goodenough, "Magnetism and the Chemical Bond" pp193-202, John Wiley and Sons, New York (1966).
51) N.Menyuk, A.Wold, D.Rogers and K.Dwight, J. Appl. Phys., 33, 1144 (1962).
52) K.Dwight, N.Menyuk, D.B.Rogers and A.Wold, Proceedings of the International Conf. on Magnetism, Nuttingham, Sept. 1964.

ACKNOWLEDGEMENTS

The authour wishes to gratefully acknowledge Prof. T. Katsura for many useful advices and his interest throughout this study.

He also wishes to thank Prof. Y. Shimizu of Meiji University for his instruction on practical measurements of magnetism and for kind suggestions. In addition, he is indebted to Prof. S. Akimoto and Dr. Y. Shono, University of Tokyo, and the members of the Katsura Laboratory, Tokyo Institute of Technology, for their valuable discussions and suggestions during this study.